basis of these observations, we termed these derived cells mouse iPS cell-derived NCLC. Further, we examined the expression of DMC markers Lhx6, Msx1, and Pax9, and the odontoblast marker DSP, [13,14,23,24], in the NCLC by immunofluorescence. Although Lhx6, Msx1, and Pax9 are expressed in cells other than dental mesenchyme, the combined expression of these genes is specific to DMC [25]. Lhx6 and Msx1 were detected in the NCLC, whereas Pax 9 and DSP were not (Fig. 3).

Further, to evaluate their tumorigenicity we subcutaneously injected NCLC into immunodeficient mice. After 4 weeks, these transplanted NCLC did not form visible teratomas (Fig. 4A), as expected from the absence of Nanog expression; whereas parental undifferentiated iPS formed teratomas including those containing various types of tissues such as bone, cartilage, epidermis, muscle, adipose tissue, and gut-like epithelium (Fig. 4A, B). To further confirm that the NCLC did not form tumors, we performed in vivo imaging to assess tumor angiogenesis. The mice injected with undifferentiated iPS cells showed significant fluorescence of the blood pool-imaging agent at the teratoma site, whereas the NCLC-injected ones showed no imaging signals, indicating the absence of a tumor.

Together, these results suggest that we could obtain nontumorigenic NCLC efficiently from mouse iPS cells by using this protocol.

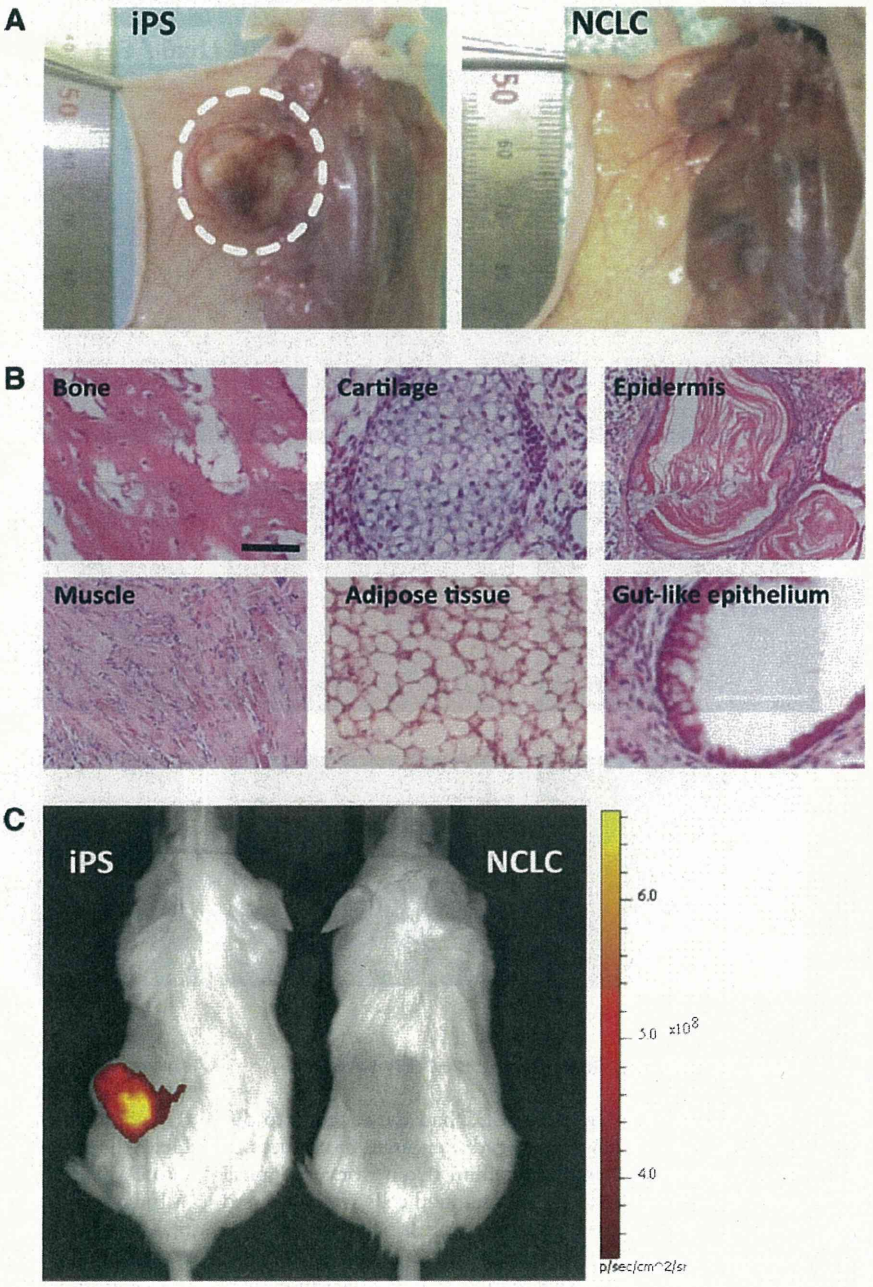

FIG. 4. Teratoma formation of NCLC. **(A)** Tumor monitoring 4 weeks after the injection of NCLC (*right*) into nude mice compared with that after injection of undifferentiated iPS cells (*left*). The *white-dotted circle* indicates the teratoma. **(B)** H-E staining of the teratoma derived from undifferentiated iPS cells. Scale bar = 50 μm. **(C)** Four weeks after mice had been subcutaneously injected with NCLC or undifferentiated iPS cells, Angiosence 750 was injected via a tail vein. A representative mouse injected with undifferentiated iPS cells (*left*) shows significant fluorescence at the teratoma site, whereas the NCLC-injected mouse (*right*) shows no imaging signals. H-E, hematoxylin and eosin. Color images available online at www.liebertonline.com/scd

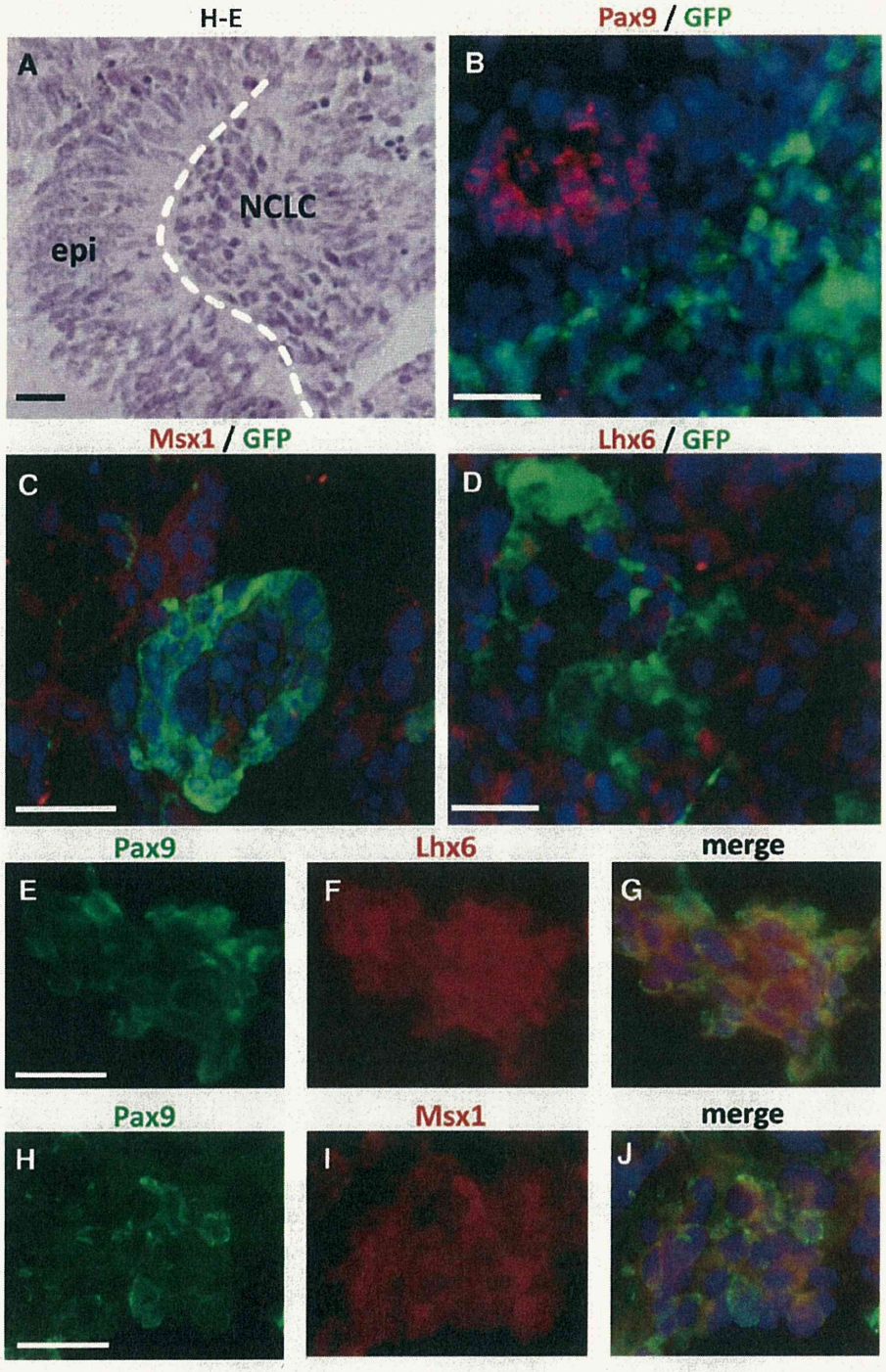

FIG. 5. Combination cultures of NCLC and dental epithelium. **(A)** The image shows an H-E stained 2-week culture. The *white-dotted line* indicates the border between NCLC and dental epithelium (epi). **(B–D)** The cultures were double-stained with the indicated antibodies. GFP-expressing dental epithelium did not express DMC markers. **(E–J)** Pax9 was co-localized with Lhx6 **(E–G)** or Msx1 **(H–J)**. Nuclei are shown in *blue*. Scale bar = 20 μm. Color images available online at www.liebertonline.com/scd

Odontogenic response of iPS cell-derived NCLC

To determine whether the NCLC had the capacity to differentiate into DMC, we prepared combination cultures of NCLC and mouse dental epithelium taken from the apical ends of the lower incisors. The combined cells were cultured in vitro and analyzed for the expression of molecular markers of tooth development. After 2 weeks in culture, NCLC aggregation adjacent to the dental epithelium was observed (Fig. 5A). Pax9, Msx1, and Lhx6 were expressed in the NCLC but not in the GFP-expressing dental epithelium (Fig. 5B–D), and Pax9 was co-expressed with Msx1 and Lhx6 (Fig. 5E–J), suggesting the differentiation of NCLC into DMC.

Interestingly, some NCLC also expressed the odontoblast marker DSP (Fig. 6A). In contrast, no marker expression was observed in combination cultures of undifferentiated iPS cells and dental epithelium (data not shown). Additionally,

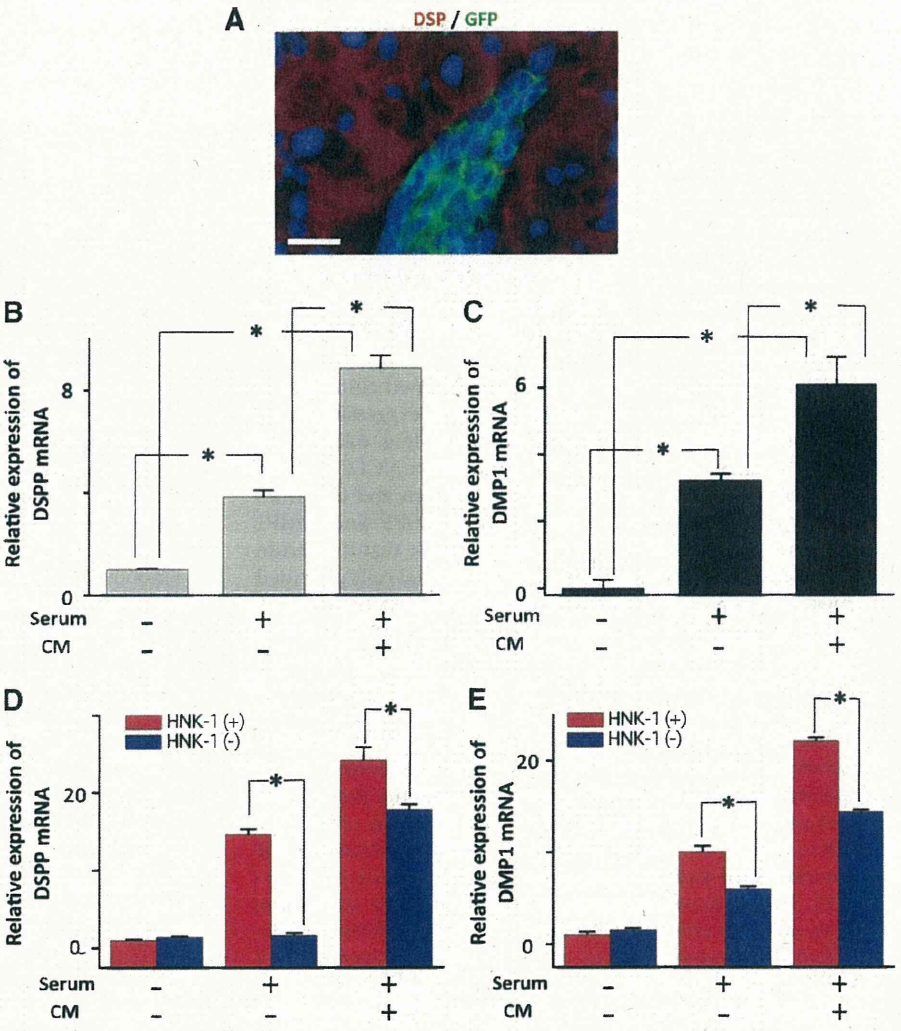

FIG. 6. Odontogenic response of NCLC to dental epithelium. **(A)** Cultures of NCLC combined with GFP-expressing dental epithelium were double-stained with DSP and GFP antibodies. Dental epithelium did not express DSP. Nuclei are shown in *blue*. Scale bar = 10 μm. **(B** and **C)** DSPP and DMP1 mRNA expression of NCLC after 2 weeks of culture with serum or conditioned medium (CM) from cultures of dental epithelial cells. **(D** and **E)** DSPP and DMP1 mRNA expression of HNK-1 positive (+) and HNK-1 negative (−) cells isolated from an NCLC population and cultured for 2 weeks with serum or CM from dental epithelial cell cultures. *Asterisks* indicate significant differences (*$P < 0.05$) between values indicated by the brackets. DSP, dentin sialoprotein; DSPP, dentin sialophosphoprotein; DMP1, dentin morphological protein 1. Color images available online at www.liebertonline.com/scd

when NCLC were cultured in the presence of serum, dentin sialophosphoprotein (DSPP) and dentin morphological protein 1 (DMP1) mRNA expression increased; and this increase was further enhanced with the conditioned medium (CM) of dental epithelial cell cultures (Fig. 6B, C). Moreover, the HNK-1-positive cells isolated from the NCLC population presented higher expression of DSPP and DMP1 than the HNK-1-negative cells when cultured with serum or with CM from dental epithelial cell cultures (Fig. 6D, E). Taken together, these results indicate that iPS cell-derived NCLC, especially the HNK-1 positive cells, had the potential to differentiate into odontoblast progenitor cells upon stimulation with dental epithelium.

Discussion

In this study, we succeeded in inducing the differentiation of mouse iPS cells into NCLC in vitro, and demonstrated for the first time that NCLC could further differentiate into odontogenic mesenchymal cells, including odontoblasts progenitor cells. We modified a culture protocol for the differentiation of hESCs [17] into NC cells, and showed that it was suitable for use with mouse iPS cells, though the species (murine and primate) and cell types (iPS and ES) were different. With regard to species, the signaling pathways that regulate primate ES cell differentiation are similar to those operating in murine ES cells [25]. Therefore, this confirms the success of transferring differentiation strategies from the primate to the murine system. In fact, the method for inducing differentiation of murine ES cells into neural cells functions with primate ES cells as well [26,27]. Concerning cell types, iPS cells are virtually equivalent to ES cells in terms of pluripotency, ES cell marker expression, and teratoma formation in vivo [4–6]. Previous reports demonstrated that iPS cells differentiate into various cell types, including NC cells, under the same culture conditions as used for ES cells [7–9]. However, some reports documented that the differentiation capability of iPS cells is lower than that of ES cells [8,9]. Hence, further improvements are needed for enhancing iPS cell differentiation capacity.

Our iPS cell-derived NCLC expressed NC markers such as nestin, $p75^{NTR}$, AP2-α, and Wnt-1 (Fig. 2). However, interestingly, Foxd3 was not expressed. In Mundell's report, Foxd3 is downregulated in cranial NC mesenchyme, and Foxd3-null cranial NC cells show accelerated differentiation into mesenchymal cells [28]. Using our differentiation

protocol, we found that NCLC expressed the mesenchymal stem cell markers STRO-1, Lhx6, and Msx1, which are expressed in dental mesenchyme. Hence, NCLC may have preferentially differentiated into mesenchymal cells. In addition to Lhx6 and Msx1 expression, NCLC expressed Pax9 (Fig. 5), when cultured with dental epithelium. This result is consistent with Ohazama's report showing that ES cells, neural stem cells, and adult bone marrow-derived cells express Lhx6, Msx1, and Pax9 when cultured with embryonic oral epithelium [29]. Thus, similar to ES and other stem cells, our iPS cell-derived NCLC showed the capacity to differentiate into dental mesenchyme upon stimulation with dental epithelium.

We further showed that NCLC in combined culture with dental epithelium differentiated into DSP-expressing cells, indicating differentiation into odontoblasts (Fig. 6A). In this experiment, we detected DSP expression in NCLC around the dental epithelium. In addition, the serum and CM from dental epithelial cell cultures enhanced DSPP and DMP1 expression (Fig. 6B–E). These results suggest that the serum and soluble components from dental epithelial cells provided NCLC with an environment suitable for odontoblast differentiation. Since NCLC derived from hESCs differentiate into several mesenchymal lineages in the presence of serum [15], our iPS cells-derived NCLC may have been induced to differentiate into DMC lineages in the presence of serum and further to differentiate into odontoblasts in the presence of soluble components of the dental epithelium. Medium conditioned by tooth germs or ameloblasts has the potential to induce stem cells to differentiate into odontogenic cells [1,30]. Thus, CM, including ours, may contain important signal molecules for tooth development, such as Notch-1 and FGFs [20]. Further investigation is needed to identify the factors that promote effective odontoblast induction. Since the detailed mechanism of the spatio-temporal regulation of odontoblast differentiation is still unclear, our culture protocol will be most useful for studying odontoblast differentiation. In addition to odontoblasts, dental pulp cells and dental follicle cells are also believed to arise from DMC during tooth germ development. Although not addressed here, it would be interesting to know whether NCLC have the capability to differentiate into those 2 cell types.

Recent advances in tissue engineering techniques indicate that the bioengineering approach may be successful for the regeneration of dental tissue. The main concept of tooth regeneration is to mimic the process of natural tooth development, either in vitro or in vivo. By taking advantage of reciprocal epithelial–mesenchymal interactions, numerous studies have shown that dental epithelial and mesenchymal cells in fetal tooth germs can form bioengineered teeth [31–33]. However, regarding clinical applications, the use of fetal tissue and/or cells gives rise to the same ethical issues as those encountered with ES cells. Therefore, iPS cell-derived DMC generated in this study have the potential to overcome the problems related to cell sources for stem cell-based tooth regeneration and treatment of tooth-related diseases.

Acknowledgments

This work was supported, in part, by the Iwate Medical University Open Research Project (2007–2011; to K.O., N.F., and H.H.), by grants from the programs Grants-in-Aid for Scientific Research (C; No. 19562128 to N.F.) and Grants-in-Aid for Young Scientists (C; No. 20679006 to S.F.) from MEXT, and by the Next Program LS010 (to S.F.)

Author Disclosure Statement

No competing financial interests exist.

References

1. Huo N, L Tang, Z Yang, H Qian, Y Wang, C Han, Z Gu, Y Duan and Y Jin. (2010). Differentiation of dermal multipotent cells into odontogenic lineage induced by embryonic and neonatal tooth germ cell-conditioned medium. Stem Cells Dev 19:93–104.
2. Yu J, Z Deng, J Shi, H Zhai, X Nie, H Zhuang, Y Li and Y Jin. (2006). Differentiation of dental pulp stem cells into regular-shaped dentin-pulp complex induced by tooth germ cell conditioned medium. Tissue Eng 12:3097–3105.
3. Miura M, S Gronthos, M Zhao, B Lu, LW Fisher, PG Robey and S Shi. (2003). SHED: stem cells from human exfoliated deciduous teeth. Proc Natl Acad Sci U S A 100:5807–5812.
4. Okita K, T Ichisaka and S Yamanaka. (2007). Generation of germline-competent induced pluripotent stem cells. Nature 448:313–317.
5. Takahashi K and S Yamanaka. (2006). Induction of pluripotent stem cells from mouse embryonic and adult fibroblast cultures by defined factors. Cell 126:663–676.
6. Takahashi K, K Tanabe, M Ohnuki, M Narita, T Ichisaka, K Tomoda and S Yamanaka. (2007). Induction of pluripotent stem cells from adult human fibroblasts by defined factors. Cell 131:861–872.
7. Chambers SM, CA Fasano, EP Papapetrou, M Tomishima, M Sadelain and L Studer. (2009). Highly efficient neural conversion of human ES and iPS cells by dual inhibition of SMAD signaling. Nat Biotechnol 27:275–280.
8. Mauritz C, K Schwanke, M Reppel, S Neef, K Katsirntaki, LS Maier, F Nguemo, S Menke, M Haustein, J Hescheler, G Hasenfuss and U Martin. (2008). Generation of functional murine cardiac myocytes from induced pluripotent stem cells. Circulation 118:507–517.
9. Morizane R, T Monkawa and H Itoh. (2009). Differentiation of murine embryonic stem and induced pluripotent stem cells to renal lineage in vitro. Biochem Biophys Res Commun 390:1334–1339.
10. Thesleff I and P Sharpe. (1997). Signalling networks regulating dental development. Mech Dev 67:111–123.
11. Jernvall J and I Thesleff. (2000). Reiterative signaling and patterning during mammalian tooth morphogenesis. Mech Dev 92:19–29.
12. Imai H, N Osumi-Yamashita, Y Ninomiya and K Eto. (1996). Contribution of early-emigrating midbrain crest cells to the dental mesenchyme of mandibular molar teeth in rat embryos. Dev Biol 176:151–165.
13. Satokata I and R Maas. (1994). Msx1 deficient mice exhibit cleft palate and abnormalities of craniofacial and tooth development. Nat Genet 6:348–356.
14. Peters H, A Neubuser, K Kratochwil and R Balling. (1998). Pax9-deficient mice lack pharyngeal pouch derivatives and teeth and exhibit craniofacial and limb abnormalities. Genes Dev 12:2735–2747.
15. Lee G, H Kim, Y Elkabetz, G Al Shamy, G Panagiotakos, T Barberi, V Tabar and L Studer. (2007). Isolation and directed differentiation of neural crest stem cells derived from human embryonic stem cells. Nat Biotechnol 25:1468–1475.

16. Bajpai R, G Coppola, M Kaul, M Talantova, F Cimadamore, M Nilbratt, DH Geschwind, SA Lipton and AV Terskikh. (2009). Molecular stages of rapid and uniform neuralization of human embryonic stem cells. Cell Death Differ 16:807–825.
17. Bajpai R, DA Chen, A Rada-Iglesias, J Zhang, Y Xiong, J Helms, CP Chang, Y Zhao, T Swigut and J Wysocka. (2010). CHD7 cooperates with PBAF to control multipotent neural crest formation. Nature 463:958–962.
18. Akimoto T, N Fujiwara, T Kagiya, K Otsu, K Ishizeki and H Harada. (2011). Establishment of Hertwig's epithelial root sheath cell line from cells involved in epithelial-mesenchymal transition. Biochem Biophys Res Commun 404:308–312.
19. Otsu K, S Das, SD Houser, SK Quadri, S Bhattacharya and J Bhattacharya. (2009). Concentration-dependent inhibition of angiogenesis by mesenchymal stem cells. Blood 113:4197–4205.
20. Harada H, P Kettunen, HS Jung, T Mustonen, YA Wang and I Thesleff. (1999). Localization of putative stem cells in dental epithelium and their association with Notch and FGF signaling. J Cell Biol 147:105–120.
21. Kawano S, T Morotomi, T Toyono, N Nakamura, T Uchida, M Ohishi, K Toyoshima and H Harada. (2002). Establishment of dental epithelial cell line (HAT-7) and the cell differentiation dependent on Notch signaling pathway. Connect Tissue Res 43:409–412.
22. Chai Y, X Jiang, Y Ito, P Bringas, Jr., J Han, DH Rowitch, P Soriano, AP McMahon and HM Sucov. (2000). Fate of the mammalian cranial neural crest during tooth and mandibular morphogenesis. Development 127:1671–1679.
23. Grigoriou M, AS Tucker, PT Sharpe and V Pachnis. (1998). Expression and regulation of Lhx6 and Lhx7, a novel subfamily of LIM homeodomain encoding genes, suggests a role in mammalian head development. Development 125:2063–2074.
24. Yamakoshi Y, JC Hu, T Iwata, K Kobayashi, M Fukae and JP Simmer. (2006). Dentin sialophosphoprotein is processed by MMP-2 and MMP-20 in vitro and in vivo. J Biol Chem 281:38235–38243.
25. Murry CE and G Keller. (2008). Differentiation of embryonic stem cells to clinically relevant populations: lessons from embryonic development. Cell 132:661–680.
26. Kawasaki H, K Mizuseki, S Nishikawa, S Kaneko, Y Kuwana, S Nakanishi, SI Nishikawa and Y Sasai. (2000). Induction of midbrain dopaminergic neurons from ES cells by stromal cell-derived inducing activity. Neuron 28:31–40.
27. Kawasaki H, H Suemori, K Mizuseki, K Watanabe, F Urano, H Ichinose, M Haruta, M Takahashi, K Yoshikawa, et al. (2002). Generation of dopaminergic neurons and pigmented epithelia from primate ES cells by stromal cell-derived inducing activity. Proc Natl Acad Sci U S A 99:1580–1585.
28. Mundell NA and PA Labosky. (2011). Neural crest stem cell multipotency requires Foxd3 to maintain neural potential and repress mesenchymal fates. Development 138:641–652.
29. Ohazama A, SA Modino, I Miletich and PT Sharpe. (2004). Stem-cell-based tissue engineering of murine teeth. J Dent Res 83:518–522.
30. Ning F, Y Guo, J Tang, J Zhou, H Zhang, W Lu, Y Gao, L Wang, D Pei, Y Duan and Y Jin. (2010). Differentiation of mouse embryonic stem cells into dental epithelial-like cells induced by ameloblasts serum-free conditioned medium. Biochem Biophys Res Commun 394:342–347.
31. Nakao K, R Morita, Y Saji, K Ishida, Y Tomita, M Ogawa, M Saitoh, Y Tomooka and T Tsuji. (2007). The development of a bioengineered organ germ method. Nat Methods 4:227–230.
32. Takahashi C, H Yoshida, A Komine, K Nakao, T Tsuji and Y Tomooka. (2010). Newly established cell lines from mouse oral epithelium regenerate teeth when combined with dental mesenchyme. In Vitro Cell Dev Biol Anim 46:457–468.
33. Nait Lechguer A, ML Couble, N Labert, S Kuchler-Bopp, L Keller, H Magloire, F Bleicher and H Lesot. (2011). Cell differentiation and matrix organization in engineered teeth. J Dent Res 90:583–589.

Address correspondence to:
Prof. Hidemitsu Harada
Division of Developmental Biology and Regenerative Medicine
Department of Anatomy
Iwate Medical University
2-1-1, Nishitokuta
Yahaba 028-3694
Japan

E-mail: hideha@iwate-med.ac.jp

Received for publication April 28, 2011
Accepted after revision November 12, 2011
Prepublished on Liebert Instant Online November 15, 2011

Biochemical and Biophysical Research Communications xxx (2011) xxx–xxx

Contents lists available at ScienceDirect

Biochemical and Biophysical Research Communications

journal homepage: www.elsevier.com/locate/ybbrc

Acerogenin A, a natural compound isolated from *Acer nikoense* Maxim, stimulates osteoblast differentiation through bone morphogenetic protein action

Tasuku Kihara [a,b,c], Saki Ichikawa [a], Takayuki Yonezawa [d], Ji-Won Lee [d], Toshihiro Akihisa [e], Je Tae Woo [d], Yasuyuki Michi [b], Teruo Amagasa [b], Akira Yamaguchi [a,c,*]

[a] Section of Oral Pathology, Graduate School of Medical and Dental Sciences, Tokyo Medical and Dental University, Tokyo, Japan
[b] Section of Maxillofacial Surgery, Graduate School of Medical and Dental Sciences, Tokyo Medical and Dental University, Tokyo, Japan
[c] Global Center of Excellence (GCOE) Program, International Research Center for Molecular Science in Tooth and Bone Diseases, Tokyo Medical and Dental University, Tokyo, Japan
[d] Research Institute for Biological Functions, Chubu University, Kasugai, Aichi, Japan
[e] College of Science and Technology, Nihon University, Tokyo, Japan

ARTICLE INFO

Article history:
Received 1 February 2011
Available online xxxx

Keywords:
Acerogenin A
Natural compound
Osteoblast
BMP
Runx2
Noggin

ABSTRACT

We investigated the effects of acerogenin A, a natural compound isolated from *Acer nikoense* Maxim, on osteoblast differentiation by using osteoblastic cells. Acerogenin A stimulated the cell proliferation of MC3T3-E1 osteoblastic cells and RD-C6 osteoblastic cells (Runx2-deficient cell line). It also increased alkaline phosphatase activity in MC3T3-E1 and RD-C6 cells and calvarial osteoblastic cells isolated from the calvariae of newborn mice. Acerogenin A also increased the expression of mRNAs related to osteoblast differentiation, including *Osteocalcin*, *Osterix* and *Runx2* in MC3T3-E1 cells and primary osteoblasts: it also stimulated *Osteocalcin* and *Osterix* mRNA expression in RD-C6 cells. The acerogenin A treatment for 3 days increased *Bmp-2*, *Bmp-4*, and *Bmp-7* mRNA expression levels in MC3T3-E1 cells. Adding noggin, a BMP specific-antagonist, inhibited the acerogenin A-induced increase in the *Osteocalcin*, *Osterix* and *Runx2* mRNA expression levels. These results indicated that acerogenin A stimulates osteoblast differentiation through BMP action, which is mediated by Runx2-dependent and Runx2-independent pathways.

1. Introduction

Osteoblasts play a crucial role in bone formation. They derive from the mesenchymal stem cells and differentiate into mature and functional osteoblasts, which process is regulated by many factors. Among these factors, bone morphogenetic proteins (BMPs) are the strongest inducers of osteoblast differentiation and bone formation [1,2]. In this process, BMPs activate runt-related gene 2 (Runx2) [3], which is an essential transcription factor for osteoblast differentiation and bone formation; Runx2-deficient mice lacked bone formation because of the maturation arrest of osteoblasts [4–6]. Osterix, another transcription factor, is also essential for osteoblast differentiation and bone formation since osterix-deficient mice also lack bone formation because of the maturation arrest of osteoblasts [7]. These two transcription factors govern the critical regulation of osteoblast differentiation and bone formation. Runx2 is more upstream factor than osterix during osteoblast differentiation and bone formation because Runx2-deficient mice do not exhibits osterix expression but osterix-deficient mice retain-Runx2 expression in their skeletal tissue [7]. Thus, osteoblast differentiation and bone formation are critically regulated by BMPs and the transcription factors, Runx2 and osterix, which regulate the expression of the osteoblast-related genes encoding alkaline phosphatase (ALP), type I collagen and osteocalcin [2].

BMPs were originally identified as proteins that induced ectopic bone formation when implanted into muscular tissue, and these play important roles in bone regeneration [1,8]. Several lines of evidence have shown that the BMP expression levels are upregulated during bone regeneration, and that BMPs stimulate osteoblast differentiation and bone regeneration [9–13]. Therefore, BMPs are suitable for therapeutic use in bone repair and BMPs have been used for human bone regeneration therapy [14–16]. In addition, chemicals or drugs that upregulate BMP expression will be useful for developing therapeutic drugs for bone regeneration [17–20].

Some natural compounds exert anabolic effects on bone metabolism [21]. We performed extensive screening for identifying new natural compounds that stimulate osteoblast differentiation and identified several such candidates. In the present study, we have investigated the effects of one of these compounds, acerogenin A (ACE), on osteoblast differentiation. ACE was isolated from *Acer nikoense* Maxim, which is indigenous to Japan and its stem bark has been used in folk medicine as a remedy for hepatic disorders

* Corresponding author at: Section of Oral Pathology, Graduate School of Medical and Dental Sciences, Tokyo Medical and Dental University, 1-5-45 Yushima, Bunkyo-ku, Tokyo 113-8549, Japan. Fax: +81 3 5803 0188.
E-mail address: akira.mpa@tmd.ac.jp (A. Yamaguchi).

0006-291X/$ - see front matter © 2011 Elsevier Inc. All rights reserved.
doi:10.1016/j.bbrc.2011.02.017

and eyewash [22]. Many new diarylheptanoids and their glycosides named acerogenin and aceroside were isolated from the stem bark of *A. nikoense*. Nagai et al. first isolated ACE from the stem bark of *A. nikoense* in 1976 [23], and many structurally related products have been identified. These compounds exert several biological actions including the inhibitory effects of degranulation in basophilic leukemia cells [24], the protective effects against hepatic injury [25], the inhibitory effects on nitric oxide production in lipopolysaccharide-activated macrophages [26] and the inhibitory effect of Na^+-glucose cotransporter [27], which is a specific activity of ACE. However, its beneficial effects on osteoblast differentiation have not been evaluated.

To investigate the effects of ACE, we used three kinds of osteoblastic cells, MC3T3-E1 cells, RD-C6 cells and calvarial osteoblastic cells. The MC3T3-E1 cell line is a typical osteoblastic cell lines isolated from mouse calvariae. RD-C6 cells are isolated from Runx2-deficient mouse embryos [28]. We have previously reported that RD-C6 cells are capable of differentiating into certain stages of osteoblasts by stimulation with BMP-2, indicating the usefulness of this cell line for identifying the molecular events underlying osteoblast differentiation through the Runx2-independent pathway [28]. Calvarial osteoblastic cells retain osteoblastic characteristics well and these cells are used as primary osteoblastic cells [29].

In this study, we found that ACE stimulates osteoblast differentiation through BMP action, which is mediated by both Runx2-dependent and Runx2-independent pathways. These results indicate that ACE is a potent compound that stimulates osteoblast differentiation and suggest that ACE is a potential candidate for therapeutic use in bone regeneration as an agent for stimulating bone formation.

2. Materials and methods

2.1. Reagents

Acerogein A (ACE) was provided from Dr. Toshihiro Akihisa. Recombinant mouse noggin was purchased from R&D Systems (Minneapolis, MN). Specific PCR primers for mouse *Alp*, *Osteocalcin (Ocn)*, *Osterix*, *Runx2*, *Bmp-2*, *Bmp-4*, *Bmp-7* and *18s RNA* were synthesized by BEX Co., Ltd. (Tokyo, Japan). All other chemicals and reagents were of analytical grade.

2.2. Cell culture

MC3T3-E1 osteoblastic cells were purchased from Cell Bank, RIKEN BioResource Center (Tsukuba, Japan). The Runx2-deficient cell line, RD-C6, was isolated from Runx2-deficient mouse embryos as described previously [28]. Primary osteoblastic cells (calvarial cells) were isolated from the calvariae of newborn C57B/6 J mice. The cells were inoculated into 24-well plates at a density of 2.5×10^4 cells/well, except for cell proliferation assay. These cells were cultured using α-modified minimum essential medium containing 10% fetal bovine serum (Sigma, St. Louis, MO), 50 units/ml penicillin G and 50 mg/ml streptomycin.

2.3. Cell proliferation assay

MC3T3-E1 cells and RD-C6 cells were inoculated into 24-well plates at a cell density of 250 cells/well and 500 cells/well, respectively, and cultured with or without 30 μM of ACE up to day 6. The cell number for each cell type was assessed on days 2, 4, and 6 after cell inoculation. The cell number was counted on removing the cells after incubation with calcium and magnesium free-phosphate buffered saline containing 0.25% trypsin and 0.04%ethylenediaminetetraacetic acid. The doubling time for each cell type was estimated using cell counts obtained during the culture.

2.4. Measurement of alkaline phosphatase activity and histochemical staining

Cultured cells were sonicated in radioimmunoprecipitation assay (RIPA) buffer to obtain cell lysate. ALP activity was determined using *p*-nitrophenylphosphate solution (Wako Pure Chemicals, Osaka, Japan) as the substrate [9]. For histochemical detection of ALP activity, the cultured cells were fixed in 10% phosphate-buffered formalin for 5 min, washed twice with 10 mM Tris–HCl (pH 7.5), and then stained with ALP [10].

2.5. Reverse transcriptase-polymerase chain reaction analysis

For the reverse transcriptase-polymerase chain reaction (RT-PCR) analysis, total RNA was extracted from the cultured cells by using NucleoSpin (Macherey–Nagel, Duren, Germany). RNA aliquots were reverse transcribed to complementary DNAs by using an oligo (dT) primer (Roche), deoxynucleotide triphosphate (dNTP; Promega), and Moloney murine leukemia virus (M-MuLV) reverse transcriptase (Fermentas, Hanover, MD). The complementary DNA products were subjected to PCR amplification with gene-specific primers for mouse *Osteocalcin*, *Runx2*, *Osterix*, *Alp*, *Bmp-2*, *Bmp-4*, and *Bmp-7* (Table 1). Real-time RT-PCR amplification was performed using a LightCycler System (Roche) with a Platinum SYBR Green qPCR SuperMix UDG kit (Invitrogen, Carlsbad, CA). The relative amount of each mRNA in each sample was normalized to the18S rRNA level.

2.6. Statistical analyses

We used analysis of variance with an F-test, followed by a t-test. *P* values less than 0.05 were considered significant. The data are presented as mean ± standard deviation values of independent replicates.

3. Results

3.1. Effective doses of ACE for osteoblast differentiation

Because ALP is an early-stage marker and osteocalcin is a late-stage marker for osteoblast differentiation, we first tested the dose–response effects of ACE on *Alp* and *Osteocalcin* mRNA expres-

Tabe1
Primer sequences of RT-PCR.

Gene	Forward	Reverse
Alkaline phosphatase	5′-TGAGCGACACGGACAAGA	3′-GGCCTGGTAGTTGTTGTGAG
Osteocalcin	5′-CCAAGCAGGAGGGCAATA	3′-AGGGCAGCACAGGTCCTAA
Osterix	5′-TATGCTCCGACCTCCTCAACT	3′-TCCTATTTGCCGTTTTCCCGA
Runx2	5′-ATCCATCCAACTCCACCACG	3′-AGAGGAAGGCCAGAGGCA
BMP-2	5′-CCCCAAGACACAGTTCCCTA	3′-GAGACCGCAGTCCGTCTAAG
BMP-4	5′-TGAGCCTTTCCAGCAAGTTT	3′-CTTCCCGGTCTCAGGTATCA
BMP-7	5′-GAAAACAGCAGCAGTGACCA	3′-GGTGGCGTTCATGTAGGAGT
18S rRNA	5′-GTAACCCGTTGAACCCCATT	3′-CCATCCAATCGGTAGTAGCG

Please cite this article in press as: T. Kihara et al., Acerogenin A, a natural compound isolated from *Acer nikoense* Maxim, stimulates osteoblast differentiation through bone morphogenetic protein action, Biochem. Biophys. Res. Commun. (2011), doi:10.1016/j.bbrc.2011.02.017

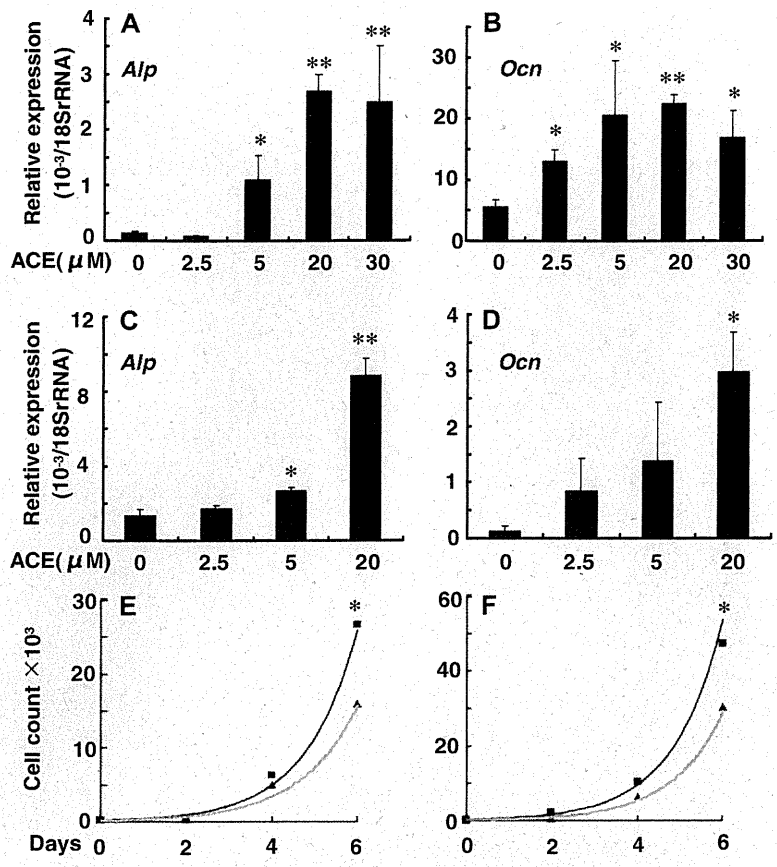

Fig. 1. Dose-dependent effects of ACE on *Alp* and *Osteocalcin* (*Ocn*) mRNA expression in MC3T3-E1 (A, B) and RD-C6 cells (C, D). These cells were treated with various concentrations of ACE for 3 days (A, B, C) or 9 days (D). Effects of ACE on the cell proliferation of MC3T3-E1 (E) and RD-C6 cells (F). Vehicle (triangle) and ACE treatment (square).The cells were cultured for 2, 4, and 6 days in the presence or absence of ACE (30 μM), and the cells numbers were assessed as described in Materials and Methods. $^{*}P < 0.05$, $^{**}P < 0.01$.

sion levels by using MC3T3-E1 and RD-C6 cells. In MC3T3-E1 cells, 3-day treatment with ACE significantly stimulated the *Alp* mRNA expression levels at 5 μM and its stimulatory effects plateauedat concentrations greater than 20 μM (Fig. 1A). *Osteocalcin* mRNA expression was significantly increased when doses greater than 2.5 μM of ACE were used (Fig. 1B). In RD-C6 cells, the *Alp* mRNA expression level significantly increased on day 3 by treatment with ACE at concentrations greater than 5 μM (Fig. 1C). Treatment with 20 μM of ACE failed to stimulate *Osteocalcin* mRNA expression during the 3-day treatment (data not shown), but when the cells were treated with the same dose, i.e., 20 μM of ACE for 9 days, the *Osteocalcin* mRNA expression level significantly increased (Fig. 1D). On the basis of these results, we performed the following experiments on the cell proliferation and differentiation of osteoblastic cells by using 30 μM of ACE.

3.2. ACE stimulated the cell proliferation of osteoblastic cells

Treatment with ACE (30 μM) did not induce any significant changes in the number of MC3T3-E1 and RD-C6 cells on days 2 and 4; however, on day 6, the number of both types of cells was significantly greater than that were not treated with ACE (Fig. 1E and F). After ACE treatment, the cell doubling times for both cell lines were lower than those for the control cultures (MC3T3-E1: control cells, 24.9 h versus ACE treated cells, 21.9 h; RD-C6: control cells, 21.4 h versus ACE treated cells, 18.4 h). These results suggest that ACE stimulates the cell proliferation of osteoblastic cells.

3.3. ACE stimulated ALP activity

Treatment with ACE for 6 days significantly increased the ALP activity in MC3T3-E1 (Fig. 2A), RD-C6 (Fig. 2C), and calvarial cells (Fig. 2E), and these stimulatory effects were also observed on ACE treatment for 21 days (Fig. 2B, D and F). The histochemical detection of ALP activity in MC3T3-E1 cells, RD-C6 cells, and calvarial cells after treatment with ACE for 6 days also indicated the stimulatory effects of ACE in these cells (data not shown).

3.4. ACE stimulated the expression of mRNAs related to osteoblast differentiation

Next, we investigated the effects of ACE on the expression of mRNAs related to osteoblast differentiation. ACE treatment for 6 days greatly increased *Alp* mRNA expression in MC3T3-E1 and RD-C6 cells (Fig. 2G and H). The 6-day ACE treatment (30 μM) significantly increased the mRNA expression level of *Osteocalcin*, which is a marker for differentiated osteoblasts, in MC3T3-E1, calvarial cells and RD-C6 cells (Fig. 3A, D and G). It also significantly enhanced the expression of *Osterix* mRNA, which encodes an essential transcription factor for osteoblast differentiation, in MC3T3-E1 cells, calvarial cells, and RD-C6 cells (Fig. 3B, E and H). ACE treatment also significantly increased the mRNA expression of *Runx2*, which encodes another essential transcription factor for osteoblast differentiation, in MC3T3-E1 and calvarial cells (Fig. 3C and F). RD-C6 cells did not express *Runx2* mRNA because these cells were isolated from Runx2-deficient mice.

Please cite this article in press as: T. Kihara et al., Acerogenin A, a natural compound isolated from *Acer nikoense* Maxim, stimulates osteoblast differentiation through bone morphogenetic protein action, Biochem. Biophys. Res. Commun. (2011), doi:10.1016/j.bbrc.2011.02.017

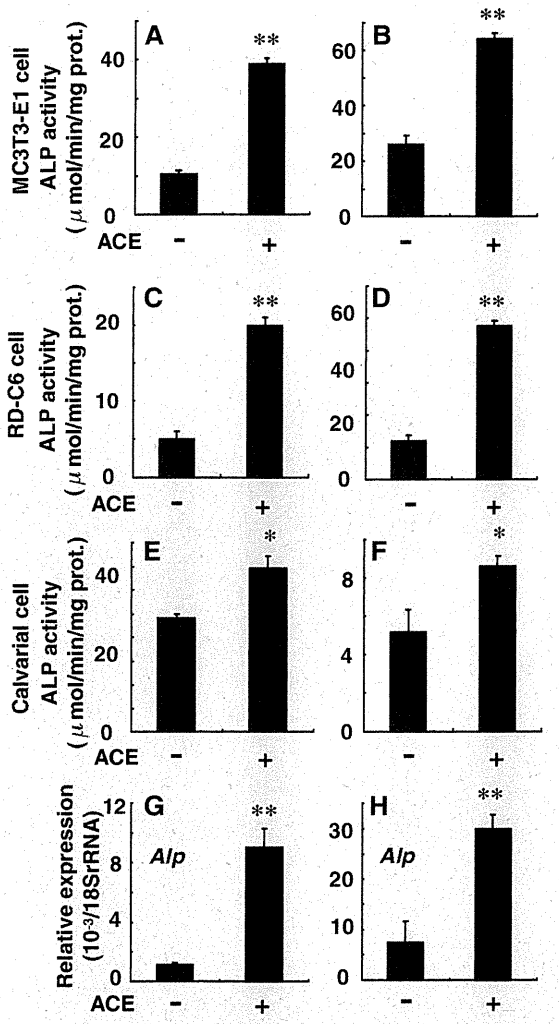

Fig. 2. Effects of ACE on ALP activity in MC3T3-E1 cells (A, B), RD-C6 cells (C, D) and calvarial cells (E, F). The cells were treated with ACE (30 μM) for 6 days (A, C, E) or 21 days (B, D, F). Effects of ACE on *Alp* mRNA expression in MC3T3-E1 (G) and RD-C6 cells (H). The cells were treated with ACE (30 μM) for 6 days, and mRNA expression was determined as described in Materials and Methods. $^{*}P < 0.05$, $^{**}P < 0.01$.

3.5. Noggin inhibited ACE-induced osteoblast differentiation

Because BMPs are the most potent inducers of osteoblast differentiation [2,9–12], we investigated the effects of noggin, a BMP specific antagonist [2,30], on ACE-induced expression of osteoblast-related mRNAs. We added noggin (500 ng/ml) to ACE-treated cultures. Noggin significantly inhibited the ACE-induced expression of *Osteocalcin* in MC3T3-E1 cells, calvarial cells, and RD-C6 cells (Fig. 3A, D and G). It also attenuated the *Osterix* mRNA expression levels in all of these cell types, but its inhibitory effects were significant in MC3T3-E1 and RD-C6 cells (Fig. 3B, E and H). This treatment also significantly inhibited the *Runx2* mRNA expression level to the control levels in MC3T3-E1 cells and calvarial cells (Fig. 3C and F). Furthermore, histochemical analysis revealed that noggin treatment inhibited ACE-induced ALP activity in MC3T3-E1, RD-C6, and calvarial cells (Fig. 3I).

3.6. ACE stimulated the expression of BMPs in osteoblastic cells

To further confirm what kinds of BMPs are involved in ACE-induced osteoblast differentiation, we evaluated *Bmp-2*, *Bmp-4* and *Bmp-7* mRNA expression after ACE treatment. After ACE (30 μM) treatment for 3 days, *Bmp-2*, *Bmp-4* and *Bmp-7* mRNA expression levels in MC3T-E1 cells were considerably higher than those in the control culture (Fig. 4A–C). Although this treatment failed to induce significant increases in the mRNA expression of these BMPs in RD-C6 cells (data not shown), ACE treatment for 6 days stimulated *Bmp-2* and *Bmp-7* mRNA expression in RD-C6 cells to levels that were significantly higher than those in control cultures (Fig. 4D and F). This treatment induced no significant increase in the *Bmp-4* mRNA level in RD-C6 cells (Fig. 4E). Treatment with ACE for 9 days significantly upregulated *Bmp4* mRNA expression in RD-C6 cells (data not shown).

3.7. ACE stimulated osteoblast differentiation in MC3T3-E1 cells in the postconfluent state

In the present study, ACE stimulated the cell proliferation of MC3T3-E1 and RD-C6 cells (Fig. 1E and F). Because the increase in cell number accelerates osteoblast differentiation *in vitro*, the effects of ACE on osteoblast differentiation may be related to the stimulated cell proliferation. To explore this possibility, we treated MC3T3-E1 cells in the postconfluent state with ACE (30 μM) for 3 days, and determined the *Alp*, *Osteocalcin*, *Osterix* and *Runx2* mRNA expression. As a result, ACE significantly increased the mRNA expression levels for *Osteocalcin*, *Osterix* and *Runx2* but not for *Alp* (Fig. 4G–J). Interestingly, the same treatment did not induce significant increases in the *Bmp2*, *Bmp4* and *Bmp7* mRNA expression levels (data not shown).

4. Discussion

In the present study, we have shown that ACE stimulated osteoblast differentiation by using MC3T3-E1 cells, RD-C6 cells, and calvarial osteoblastic cells isolated from the calvariae of newborn mice (so-called primary osteoblastic cells). We first determined the ACE doses that affected the expression of osteoblast-related genes such as *Alp* and *Osteocalcin* by using MC3T3-E1 and RD-C6 cells (Fig. 1). The results of these experiments suggested that MC3T3-E1 cells are more sensitive to ACE stimulation than are RD-C6 cells. We have also shown that ACE induces ALP activity (Fig. 2) and *Osterix*, *Runx2*, and *Osteocalcin* mRNA expression in MC3T3-E1 and calvarial cells (Fig. 4). Because Runx2 is a critical transcription factor that regulates *Osteocalcin* mRNA expression [4,6], ACE-induced increase in the *Runx2* mRNA expression level may be involved in the ACE-induced stimulatory effects on osteoblast differentiation in MC3T3-E1 and calvarial osteoblastic cells. ACE also stimulated osteoblast differentiation in RD-C6 cells, which lack Runx2 [28], by increasing the *Alp*, *Osteocalcin* and *Osterix* expression levels. These results indicate that ACE stimulates osteoblast differentiation through Runx2-dependent and Runx2-independent pathways.

To determine the mechanism underlying the stimulatory effects of ACE on osteoblast differentiation, we first investigated whether BMPs are involved in ACE-induced osteoblast differentiation, because BMPs are the most potent inducers of osteoblast differentiation; this was done using the BMP-specific antagonist, noggin. Noggin treatment significantly inhibited the ACE-induced upregulation of osteoblast-related mRNAs as well as ALP activity (Fig. 3). These results indicated that ACE-induced osteoblast differentiation is mediated by BMP action.

To explore what kinds of BMPs participated in ACE-induced osteoblast differentiation, we assessed *Bmp-2*, *Bmp-4* and *Bmp-7* mRNA expression in MC3T3-E1 and RD-C6 cells with or without ACE treatment. As expected, ACE stimulated the *Bmp-2*, *Bmp-4* and *Bmp-7* mRNA expression as early as day 3 after treatment. Be-

Please cite this article in press as: T. Kihara et al., Acerogenin A, a natural compound isolated from *Acer nikoense* Maxim, stimulates osteoblast differentiation through bone morphogenetic protein action, Biochem. Biophys. Res. Commun. (2011), doi:10.1016/j.bbrc.2011.02.017

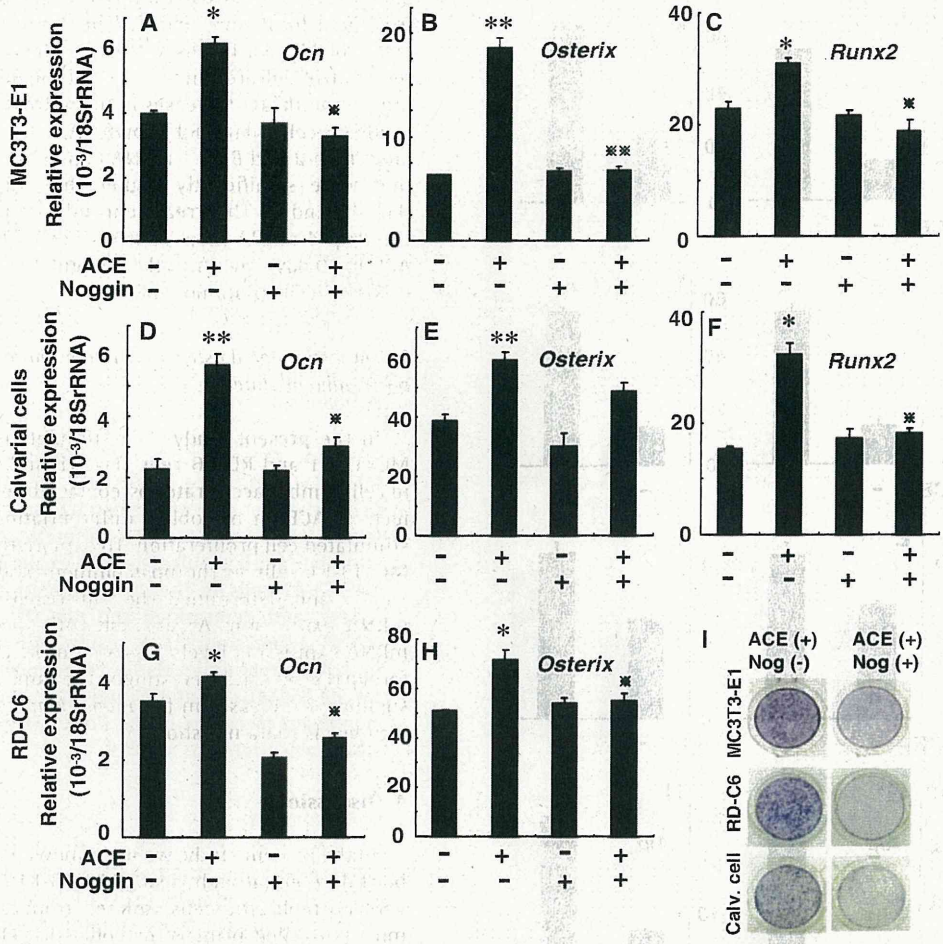

Fig. 3. Effects of ACE and noggin on *Osteocalcin* (*Ocn*), *Osterix* and *Runx2* mRNA expression in MC3T3-E1 cells (A, B, C), calvarial cells (D, E, F), and RD-C6 cells (G, H). The cells were cultured for 6 days in the presence or absence of ACE (30 μM) with or without noggin (500 ng/ml) treatment. Histochemical detection of ALP activity in MC3T3-E1 cells, RD-C6 cells and calvarial cells (I). All of the cells were treated with ACE (30 μM) for 6 days in the presence or absence of noggin (Nog), and ALP activity was detected as described in Section 2. $^{*}P < 0.05$, $^{**}P < 0.01$: significantly different from control culture [ACE (−), Noggin (−)], $\divideontimes P < 0.05$, $\divideontimes\divideontimes P < 0.01$: significantly different from ACE treated cells [ACE (+), Noggin (−)].

cause ACE treatment also stimulated *Alp* and *Osteocalcin* mRNAs expression at doses over 5 μM in MC3T3-E1 cells on day 3 after the treatment, these effects may be closely related to increase in BMP levels due to ACE treatment. In contrast, the 3-day ACE treatment induced no apparent increases in the *Bmp-2*, *Bmp-4* and *Bmp-7* mRNA expression levels in RD-C6 cells, but the 6-day treatment significantly upregulated the *Bmp-2* and *Bmp-7* mRNA expression levels in this cell line. Interestingly, ACE failed to increase *Osteocalcin* mRNA expression on day 3 after ACE treatment, but was induced on day 9 after the treatment in RD-C6 cells (Fig. 1D). These results indicate that delayed induction of *Osteocalcin* mRNA expression in RD-C6 by ACE treatment may be related to the delayed increase in BMPs expression levels in response to ACE treatment in this cell line. In contrast, ACE stimulated *Alp* mRNA expression as early as on day 3 after the treatment in RD-C6 cells (Fig. 1C). This suggests that RD-C6 cells produced BMPs other than BMP-2, BMP-4, and BMP-7 in response to ACE or that a signaling pathway other than the BMP signaling is involved in this anabolic action. The Wnt/β-catenin signaling pathway is one such candidate because this signaling pathway plays a crucial role in osteoblast differentiation [31]. Whether Wnt/β-catenin signaling is involved in ACE-induced osteoblast differentiation is of considerable interest and is under investigation in our group. These studies will provide important information for identifying the target molecules of ACE in osteoblast differentiation.

The occurrence of osteoblast differentiation depends on the cell number in *in vitro* cell culture systems. Since ACE stimulated the proliferation of osteoblastic cells, we investigated whether the stimulatory effects of ACE on osteoblast differentiation occurred in MC3T3-E1 cells in the postconfluent state. The results of this experiment revealed that ACE stimulated osteoblast differentiation even after the postconfluent stage by increasing *Osteocalcin*, *Osterix*, and *Runx2* mRNA expression, although an early differentiation marker, *Alp* mRNA expression, was not stimulated. Interestingly, the induction of BMPs by ACE treatment was not apparent compared to that observed in proliferating-stage cultures of MC3T3-E1 cells (Fig. 4A–C). These results suggested that the stimulatory effects of ACE on osteoblast differentiation partly depend on the cell proliferation effect of ACE, and that ACE-induced BMP induction preferentially occurred at a cell proliferation stage.

In summary, this is the first study to show that a natural compound, ACE, isolated from *A. nikoense* Maxim exerts stimulatory effects on osteoblast differentiation through BMP action mediated by Runx2-dependent and Runx2-independent pathways. These results suggest that ACE is a candidate anabolic agent for stimulating bone formation. This effect of ACE treatment will be useful with re-

Please cite this article in press as: T. Kihara et al., Acerogenin A, a natural compound isolated from *Acer nikoense* Maxim, stimulates osteoblast differentiation through bone morphogenetic protein action, Biochem. Biophys. Res. Commun. (2011), doi:10.1016/j.bbrc.2011.02.017

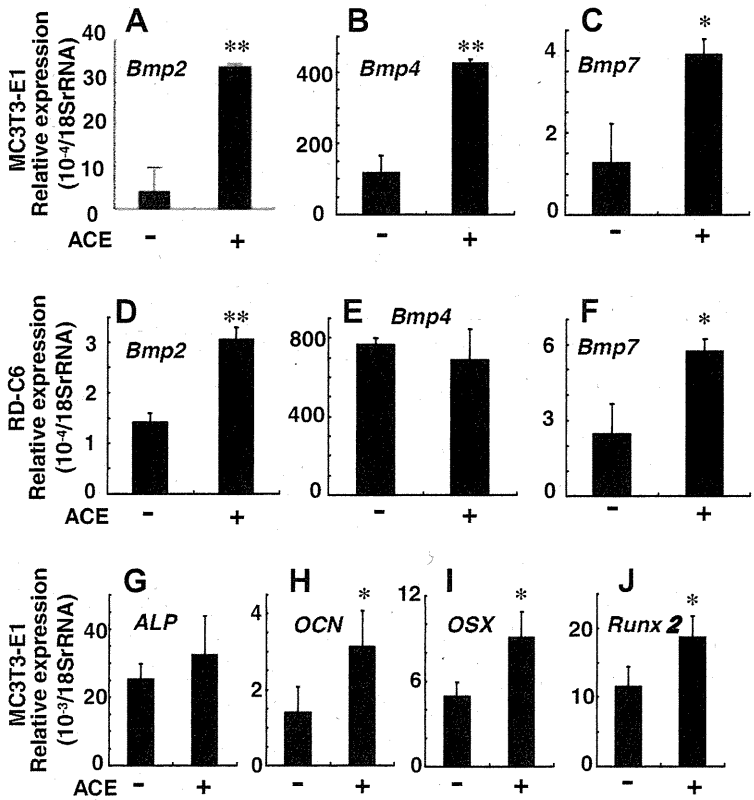

Fig. 4. A-F: Effects of ACE on *Bmp2*, *Bmp4* and *Bmp7* mRNA expression in MC3T3-E1 (A, B, C) and RD-C6 cells (D, E, F). MC3T3-E1 cells (A, B, C) were treated with ACE (30 μM) for 3 days, while RD-C6 cells (D, E, F) were treated for 6 days. G-J: Effects of ACE on *Alp*, *Osteocalcin* (*Ocn*), *Osterix*, and *Runx2* mRNA expression levels in MC3T3-E1 cells in the postconfluent state (G-I). ACE (30 μM) was added into the MC3T3-E1 cell culture on day 3 (confluent state), and mRNA expression was assessed after 3 days of the treatment. $^{*}P < 0.05$, $^{**}P < 0.01$.

gard to developing therapeutic agents for bone diseases such as bone repair and osteoporosis.

Acknowledgments

This work was supported by a Grant-in-Aid for Scientific Research from the Japan Society for the Promotion of Science (Nos. 22249061 and 21659420) and Health and Labour Sciences Research Grants from the Ministry of Health, Labour, and Welfare (No. 21040101) to A.Y., and by the Global Center of Excellence (GCOE) Program; International Research Center for Molecular Science in Tooth and Bone Diseases, Tokyo Medical and Dental University.

References

[1] J.M. Wozney, V. Rosen, A.J. Celeste, L.M. Mitsock, M.J. Whitters, R.W. Kriz, R.M. Hewick, E.A. Wang, Novel regulators of bone formation: molecular clones and activities, Science 242 (1988) 1528–1534.

[2] A. Yamaguchi, T. Komori, T. Suda, Regulation of osteoblast differentiation mediated by bone morphogenetic proteins, hedgehogs, and Cbfa1, Endocr. Rev. 21 (2000) 393–411.

[3] M.H. Lee, Y.J. Kim, H.J. Kim, H.D. Park, A.R. Kang, H.M. Kyung, J.H. Sung, J.M. Wozney, H.M. Ryoo, BMP-2-induced Runx2 expression is mediated by Dlx5, and TGF-beta 1 opposes the BMP-2-induced osteoblast differentiation by suppression of Dlx5 expression, J. Biol. Chem. 278 (2003) 34387–34394.

[4] T. Komori, H. Yagi, S. Nomura, A. Yamaguchi, K. Sasaki, K. Deguchi, Y. Shimizu, R.T. Bronson, Y.-H. Gao, M. Inada, M. Sato, R. Okamoto, Y. Kitamura, S. Yoshiki, T. Kishimoto, Targeted disruption of Cbfa1 results in a complete lack of bone formation owing to maturational arrest of osteoblasts, Cell 89 (1997) 755–764.

[5] F. Otto, A.P. Thornell, T. Crompton, A. Denzel, K.C. Gilmour, I.R. Rosewell, G.W. Stamp, R.S. Beddington, S. Mundlos, B.R. Olsen, P.B. Selby, M.J. Owen, Cbfa1, a candidate gene for cleidocranial dysplasia syndrome, is essential for osteoblast differentiation and bone development, Cell 89 (1997) 765–771.

[6] P. Ducy, R. Zhang, V. Geoffroy, A.L. Ridall, G. Karsenty, Osf2/Cbfa1: a transcriptional activator of osteoblast differentiation, Cell 89 (1997) 747–754.

[7] K. Nakashima, X. Zhou, G. Kunkel, Z. Zhang, J.M. Deng, R.R. Behringer, B. De Crombrugghe, The novel zinc finger-containing transcription factor osterix is required for osteoblast differentiation and bone formation, Cell 108 (2002) 17–29.

[8] M.R. Urist, Bone: formation by autoinduction, Science 150 (1965) 893–899.

[9] A. Yamaguchi, T. Katagiri, T. Ikeda, J.M. Wozney, V. Rosen, E.A. Wang, A.J. Kahn, T. Suda, S. oshiki, Recombinant human bone morphogenetic protein-2 stimulates osteoblastic maturation and inhibits myogenic differentiation in vitro, J. Cell Biol. 113 (1991) 681–687.

[10] T. Katagiri, A. Yamaguchi, K. Komaki, E. Abe, N. Takahashi, T. Ikeda, V. Rosen, J.M. Wozney, A. Fujisawa-Sehara, T. Suda, Bone morphogenetic protein-2 converts the differentiation pathway of C2C12 myoblasts into the osteoblast lineage, J. Cell Biol. 127 (1994) 1755–1766.

[11] A. Yamaguchi, T. Ishizuya, N. Kintou, Y. Wada, T. Katagiri, J.M. Wozney, V. Rosen, S. Yoshiki, Effects of BMP-2, BMP-4 and BMP-6 on osteoblast differentiation of bone marrow-derived stromal cell lines, ST2 and MC3T3-G2/PA6, Biochem. Biophys. Res. Commun. 220 (1996) 366–371.

[12] T.K. Sampath, J.C. Maliakal, P.V. Hauschka, W.K. Jones, H. Sasak, R.F. Tucker, K.H. White, J.E. Coughlin, M.M. Tucker, R.H.L. Pang, C. Corbett, E. Ozkaynak, H. Oppermann, D.C. Rueger, Recombinant human osteogenic protein-1 (hOP-1) induces new bone formation in vivo with a specific activity comparable with natural bovine osteogenic protein and stimulates osteoblast proliferation and differentiation in vitro, J. Biol. Chem. 267 (1992) 20352–20362.

[13] I.R. Garrett, Anabolic agents and the bone morphogenetic protein pathway, Curr. Top. Dev. Biol. 78 (2007) 127–171.

[14] A.P. White, A.R. Vaccaro, J.A. Hall, P.G. Whang, B.C. Friel, M.D. McKee, Clinical applications of BMP-7/OP-1 in fractures, nonunions and spinal fusion, Int. Orthop. 31 (2007) 735–741.

[15] H.A. Awad, X. Zhang, D.G. Reynolds, R.E. Guldberg, R.J. O'Keefe, E.M. Schwarz, Recent advances in gene delivery for structural bone allografts, Tissue Eng. 13 (2007) 1973–1985.

[16] P.C. Bessa, M. Casal, R.L. Reis, Bone morphogenetic proteins in tissue engineering: the road from laboratory to clinic, part II (BMP delivery), J. Tissue Eng. Regen. Med. 2 (2008) 81–96.

Please cite this article in press as: T. Kihara et al., Acerogenin A, a natural compound isolated from *Acer nikoense* Maxim, stimulates osteoblast differentiation through bone morphogenetic protein action, Biochem. Biophys. Res. Commun. (2011), doi:10.1016/j.bbrc.2011.02.017

[17] K. Nakagawa, Y. Imai, Y. Ohta, K. Takaoka, Prostaglandin E2 EP4 agonist (ONO-4819) accelerates BMP-induced osteoblastic differentiation, Bone 41 (2007) 543–548.

[18] T. Namikawa, H. Terai, M. Hoshino, M. Kato, H. Toyoda, K. Yano, H. Nakamura, K. Takaoka, Enhancing effects of a prostaglandin EP4 receptor agonist on recombinant human bone morphogenetic protein-2 mediated spine fusion in a rabbit model, Spine 32 (2007) 2294–2299.

[19] G. Mundy, R. Garrett, S. Harris, J. Chan, D. Chen, G. Rossini, B. Boyce, M. Zhao, G. Gutierrez, Stimulation of bone formation in vitro and in rodents by statins, Science 286 (1999) 1946–1949.

[20] G. Luisetto, V. Camozzi, Statins, fracture risk, and bone remodeling, J. Endocrinol. Invest. 32 (2009) 32–37.

[21] H. Hojo, K. Igawa, S. Ohba, F. Yano, K. Nakajima, Y. Komiyama, T. Ikeda, A.C. Lichtler, J.T. Woo, T. Yonezawa, T. Takato, U.I. Chung, Development of high-throughput screening system for osteogenic drugs using a cell-based sensor, Biochem. Biophys. Res. Commun. 376 (2008) 375–379.

[22] M. Nagai, M. Kubo, M. Fujita, T. Inoue, M. Matsuo, Studies on the constituents of Aceraceae Plants. II. Structure of aceroside I, a glucose of a novel cyclic diarylheptanoids from *Acer nikoense* Maxim, Chem. Pharm. Bull. 26 (1978) 2805–2810.

[23] M. Nagai, M. Kubo, M. Fujita, T. Inoue, M. Matsuo, Acerogenin A, a novel cyclic diarylheptanoid, J. Chem. Soc. Chem. Commun. (1976) 338–339.

[24] T. Morikawa, J. Tao, K. Ueda, H. Matsuda, M. Yoshikawa, Medicinal foodstuffs. XXXI. Structures of new aromatic constituents and inhibitors of degranulation in RBL-2H3 cells from Japanese folk medicine, the stem bark of *Acer nikoense*, Chem. Pharm. Bull. 51 (2003) 62–67.

[25] M. Shinoda, S. Ohta, M. Kumasaka, M. Fujita, M. Nagai, T. Inoue, Protective effect of the bark of *Acer nikoense* on hepatic injury induced by carbon, Shoyakugaku Zasshi 40 (1986) 177–181.

[26] T. Morikawa, J. Tao, I. Toguchida, H. Matsuda, M. Yoshikawa, Structures of new cyclic diarylheptanoids and inhibitors of nitric oxide production from Japanese folk medicine *Acer nikoense*, J. Nat. Prod. 66 (2003) 86–91.

[27] H. Morita, J. Deguchi, Y. Motegi, S. Sato, C. Aoyama, J. Takeo, M. Shiro, Y. Hirasawa, Cyclic diarylheptanoids as Na^+-glucose cotransporter (SGLT) inhibitors from *Acer nikoense*, Bioorg. Med. Chem. Lett. 20 (2010) 1070–1074.

[28] T. Liu, Y. Gao, K. Sakamoto, T. Minamizato, K. Furukawa, T. Tsukazaki, Y. Shibata, K. Bessho, T. Komori, A. Yamaguchi, BMP-2 promotes differentiation of osteoblasts and chondroblasts in Runx2-deficient cell lines, J. Cell Physiol. 211 (2007) 728–735.

[29] C.G. Bellows, J.E. Aubin, J.N. Heersche, M.E. Antosz, Mineralized bone nodules formed in vitro from enzymatically released rat calvaria cell populations, Calcif. Tissue Int. 38 (1986) 143–154.

[30] V. Rosen, BMP and BMP inhibitors in bone, Ann. NY Acad. Sci. 1068 (2006) 19–25.

[31] R. Baron, G. Rawadi, S. Roman-Roman, Wnt signaling: a key regulator of bone mass, Curr. Top. Dev. Biol. 76 (2006) 103–127.

Please cite this article in press as: T. Kihara et al., Acerogenin A, a natural compound isolated from *Acer nikoense* Maxim, stimulates osteoblast differentiation through bone morphogenetic protein action, Biochem. Biophys. Res. Commun. (2011), doi:10.1016/j.bbrc.2011.02.017

J Bone Miner Metab (2011) 29:662–670
DOI 10.1007/s00774-011-0268-6

ORIGINAL ARTICLE

Comparative morphology of the osteocyte lacunocanalicular system in various vertebrates

Lei Cao · Takeshi Moriishi · Toshihiro Miyazaki · Tadahiro Iimura · Miwako Hamagaki · Ayako Nakane · Yoshihiro Tamamura · Toshihisa Komori · Akira Yamaguchi

Received: 16 June 2010 / Accepted: 15 March 2011 / Published online: 19 April 2011

Abstract Osteocytes are embedded in the bone matrix, and they communicate with adjacent osteocytes, osteoblasts, and osteoclasts through the osteocyte lacunocanalicular system. Osteocytes are believed to be essential for the maintenance of bone homeostasis because they regulate mechanical sensing and mineral metabolism in mammalian bones; however, osteocyte morphology in other vertebrates has not been well documented. We conducted a comparative study on the morphology of osteocytes and the lacunocanalicular system of the following vertebrates: two teleost fishes [medaka (*Oryzias latipes*), and zebrafish (*Danio rerio*)], three amphibians [African clawed frog (*Xenopus laevis*), black-spotted pond frog (*Rana nigromaculata*), and Japanese fire-bellied newt (*Cynops pyrrhogaster*)], two reptiles [four-toed tortoise (*Testudo horsfieldii*) and green iguana (*Iguana iguana*)], and two mammals (laboratory mouse C57BL6 and human). The distribution of the osteocyte lacunocanalicular system in all these animals was investigated using the modified silver staining and the fluorescein-conjugated phalloidin staining methods. Bones of medaka had few osteocytes (acellular bone). Bones of zebrafish contained osteocytes (cellular bone) but had a poorly developed osteocyte lacunocanalicular system. Bones of *Xenopus laevis*, a freshwater species, and of other amphibians, reptiles, and mammals contained numerous osteocytes and a well-developed lacunocanalicular system. The present study indicates that development of the osteocyte lacunocanalicular system differs between teleost fishes and land vertebrates, but this pattern is not directly related to aquatic habitat.

Keywords Osteocytes · Medaka · Zebrafish · Reptile · *Xenopus laevis*

L. Cao · T. Iimura · M. Hamagaki · Y. Tamamura · A. Yamaguchi (✉)
Oral Pathology, Graduate School of Medical and Dental Sciences, Tokyo Medical and Dental University Graduate School, 1-5-45 Yushima, Bunkyo-ku, Tokyo 113-8549, Japan
e-mail: akira.mpa@tmd.ac.jp

A. Nakane
Developmental Oral Health Science, Graduate School of Medical and Dental Sciences, Tokyo Medical and Dental University, Tokyo, Japan

T. Moriishi · T. Miyazaki · T. Komori
Department of Cell Biology, Nagasaki University Graduate School of Biomedical Sciences, Nagasaki, Japan

T. Iimura · A. Nakane · A. Yamaguchi
Global Center of Excellence Program, International Research Center for Molecular Science in Tooth and Bone Diseases, Tokyo Medical and Dental University, Tokyo, Japan

Introduction

Mammalian bones comprise three major cell types: osteoblasts, osteoclasts, and osteocytes. Osteoblasts are responsible for bone formation, and osteoclasts for bone resorption. Bone formation and resorption are critically regulated by the close interaction between osteoblasts and osteoclasts.

Osteocytes are embedded in the mineralized bone matrix, and they organize the osteocyte lacunocanalicular system by extending numerous cytoplasmic processes into the surrounding bone matrix. Osteocytes are believed to sense mechanical strain and transmit the signals to the surrounding osteocytes, osteoblasts and osteoclasts through the osteocyte lacunocanalicular system, and induce biological response in the affected cells [1–3]. Since these signals are essential to maintaining bone homeostasis, osteocytes are now considered to play the central role in

mechanical sensing in bone. Recent studies have shown that osteocytes produce a hormone, fibroblast growth factor 23 (FGF23) [4, 5], which acts on the kidney to stimulate phosphorus excretion and inhibit 1α-hydroxylation of vitamin D [6, 7]. Dentin matrix protein 1 (DMP1), a regulator of mineralization, is specifically synthesized by osteocytes [8]. These findings indicate that the osteocyte is a key cell type in bone metabolism.

Vertebrates live in various environments. The morphology and function of osteocytes might be influenced by the respective habitats because mechanical strain and mineral intake differ between aquatic and land vertebrates. Many studies have been conducted on the morphology and function of osteocytes in mammals, but very few studies have been conducted on osteocytes in fishes [9–13], amphibians [14, 15], and reptiles [16, 17]. Furthermore, the osteocyte lacunocanalicular system in the bones of fishes, amphibians, and reptiles has not been studied in detail using standardized techniques. This lack of extensive comparative research has hampered the understanding of not only the phylogeny of osteocytes but also the evolutionary changes in bone metabolism. Recently, gene-mutated medaka and zebrafish, which are mainly transgenic fishes [18–21], are available for skeletal research. Extensive studies of osteocytes in the wild-type of these fishes are important and necessary to understand the phenotypic changes observed in gene-mutated fishes.

In the present study, therefore, we attempted to compare osteocyte morphology by focusing on the osteocyte lacunocanalicular system using Schoen's silver staining and fluorescence-conjugated phalloidin staining in the bones of various mature vertebrates including teleost fishes (medaka and zebrafish), amphibians (frog and newt), reptiles (tortoise and green iguana), and mammals (mouse and human).

Materials and methods

Animals

Mature medaka (*Oryzias latipes*), zebrafish (*Danio rerio*), African clawed frog (*Xenopus laevis*), black-spotted pond frog (*Rana nigromaculata*), Japanese fire-bellied newt (*Cynops pyrrhogaster*), four-toed tortoise (*Testudo horsfieldii*), green iguana (*Iguana iguana*), and mouse (laboratory strain C57BL6) were purchased from local distributors.

Preparation of skeletal tissues

Vertebrae of medaka and zebrafish were dissected after anesthetizing the animals with 0.1% ethyl anthranilate. Femurs and thoracic vertebrae of mature frogs, newts, tortoises, iguanas, and mice were dissected after anesthetizing the animals with ethyl ether. The samples for Schoen's silver staining were fixed in 10% buffered formalin, and those for fluorescein-conjugated phalloidin staining were fixed in 4% paraformaldehyde. After washing the fixed specimens with a phosphate-buffered saline solution, they were decalcified in 20% ethylenediaminetetraacetic acid (EDTA) for 10–14 days. The decalcified specimens were embedded in paraffin to obtain paraffin sections and in optimal cutting temperature (OCT) compound (Sakura Finetek Japan, Tokyo, Japan) to obtain cryosections. Histological sections of human femurs were obtained from paraffin blocks prepared 10 years ago from autopsies conducted at Tokyo Medical and Dental University Hospital. These femur samples were fixed in 10% buffered formalin for 2 days, and embedded in paraffin after decalcification with 5% formic acid.

Histological analysis

Longitudinal sections were prepared from the vertebrae of teleost fishes. Longitudinal sections of the diaphysis of femurs and vertebrae were prepared from amphibians, reptiles, and mice. To identify the osteocyte lacunocanalicular system, the sections were stained using a modified Bodian's Protargol-S^{TM} technique (Schoen's silver staining) in accordance with the protocol described by Hirose et al. [22]. In brief, deparaffinized sections were soaked in a 1% Protargol-S^{TM} solution, and diluted in borax boric acid (pH 7.4) for 12–48 h at 37°C. After rinsing with distilled water, the reaction was enhanced by adding an aqueous solution containing 0.2% hydroquinone, 0.2% citric acid, and 0.7% nitric silver. After additional rinsing, the sections were dipped for 5 min in aqueous solution containing 2.5% anhydrous sodium sulfite, 0.5% potassium bromide, and 0.5% amidol. The sections were then treated with 1% gold chloride, and subsequently reduced by 2% oxalic acid. After rinsing with distilled water, the sections were fixed in 5% sodium thiosulfate for 5 min before hematoxylin and eosin staining. Protargol-S^{TM} was purchased from Sigma-Aldrich Corporation (St. Louis, MO, USA), and all the other chemicals used for staining were purchased from Wako Pure Chemical Industries, Ltd. (Osaka, Japan).

Staining for actin filaments with fluorescein-conjugated phalloidin

To visualize the osteocyte lacunocanalicular system, we stained the specimens for cytoskeletal actin by using fluorescein-conjugated phalloidin. Decalcified samples of vertebrae of medaka and zebrafish and femurs of each

animal were embedded in OCT compound to obtain cryosections. The femur sections (10–20 μm thick) were incubated with Alexa Fluor® 488 phalloidin (Invitrogen, Carlsbad, CA, USA) and BOBO-3 (Invitrogen) at room temperature for 2 h to stain cytoskeletal actin and nuclear DNA, respectively. Fluorescent images were observed using a laser microscope (Axioskop 2 Plus, Carl Zeiss GmbH, Jena, Germany).

Transmission electron microscopic observation

The vertebrae of mature zebrafish and the femurs of mature *Xenopus laevis* were fixed overnight in a 2.5% glutaraldehyde–2% paraformaldehyde mixture in 0.05 M cacodylate buffer (pH 7.4) at 4°C, and then decalcified in 5% EDTA. After rinsing in 0.05 M cacodylate buffer, the specimens were post-fixed with 1% osmium acid in 0.05 M cacodylate buffer (pH 7.4) for 2 h at 4°C. The specimens were then dehydrated in an ascending acetone series and embedded in Epon–Araldite resin. Ultrathin sections (80–100 nm) were cut using a Reichert Ultracut E microtome. After collagen fiber staining with OTE solution (Nisshin EM Co., Tokyo, Japan), the sections were stained with uranyl acetate and lead citrate, and examined under a Hitachi transmission electron microscope (H-7100).

Results

Distribution of osteocytes and lacunocanalicular system in teleost fishes

The vertebral columns of mature medaka and zebrafish comprise three elements: the centrum (vertebral body), the neural arch, and the hemal arch [19]. In medaka, a thin layer of osteoblastic cells was found to cover the surface of the centrum (Fig. 1a, b, d, e). Few osteocytes were observed in the centrum, neural arch, and hemal arch in medaka (Fig. 1a, b). In contrast, however, osteocytes were scattered in the centrum (Fig. 1d, e) as well as other bones of zebrafish. These osteocytes were round, oval or elongated shape, and were arranged randomly without peculiar direction in the centrum (Fig. 1d, e).

To investigate the osteocyte lacunocanalicular system in detail, we examined the vertebral sections stained with Schoen's silver staining and fluorescein-conjugated phalloidin. Medaka vertebrae showed no apparent osteocyte lacunocanalicular system by both methods (Fig. 1a–c). Zebrafish vertebrae exhibited a scarcely stained osteocyte lacunocanalicular system around the osteocytes in the Schoen's silver-stained specimens (Fig. 1d, e); however, cytoplasmic processes around the osteocytes were infrequently observed (arrow in Fig. 1f) with the number of these processes being limited to one or two per cell. Some osteocytes showed an eosinophilic area around them, and a few osteocytes were associated with one or two cytoplasmic processes extending around them (Fig. 1f). In the sections stained with fluorescein-conjugated phalloidin, some osteocytes showed very fine and short cytoplasmic processes around them, and these processes seemed to connect with the adjacent osteocyte (Fig. 1g). Interestingly, longer cytoplasmic processes were infrequently observed in some osteocytes, which seemed to correspond to the cytoplasmic processes observed in the sections stained with Schoen's silver-stained specimens (Fig. 1f). To investigate the details of the osteocyte lacunocanalicular system in zebrafish, we also observed the specimens using a transmission electron microscopy. We found that osteocytes contained poorly developed cellular organelles (Fig. 2). Some osteocytes extended a cytoplasmic process into the surrounding bone matrix (arrows in Fig. 2b–d); however, the number of these cytoplasmic processes was limited to one or two per cell. A small number of transverse cytoplasmic processes extending from the osteocytes were seen in the bone matrix (arrows in Fig. 2c), but the number of these processes was very small. Amorphous substances varying in their electron densities filled the space of many osteocyte lacunae (Fig. 2c, d).

Distribution of osteocytes and lacunocanalicular system in amphibians

The cortical bone of the femurs of mature *Xenopus laevis* contained numerous elongated osteocytes, aligned parallel to the long axis of the femur (Fig. 3a, b). The Schoen's silver staining method revealed a well-developed osteocyte lacunocanalicular system that aligned perpendicular to the long axis of the femur (Fig. 3a). Fluorescein-conjugated phalloidin staining also revealed a well-developed osteocyte lacunocanalicular system (Fig. 3b), which resembled the findings observed by Schoen's silver staining method. Vertebral osteocytes also extended many cytoplasmic processes into the surrounding bone matrix (Fig. 3c). Transmission electron microscopy showed that the osteocytes located at the outer layer of the cortical bones contained poorly developed cellular organelles (Fig. 4a, b). These cells extended many cytoplasmic processes into the surrounding bone matrix (Fig. 4a, b). In the mid-region of the cortical bones, the osteocytes also exhibited numerous cytoplasmic processes extending into the surrounding bone matrix (Fig. 4c). Some osteocyte lacunae contained shrunken osteocytes with condensed heterochromatin in the nuclei, although osteocyte canaliculi were evident in the surrounding bone matrix (Fig. 4c, d). Since we could not find apparent apoptotic bodies in the osteocyte lacunae containing the shrunken osteocytes, we believe that the

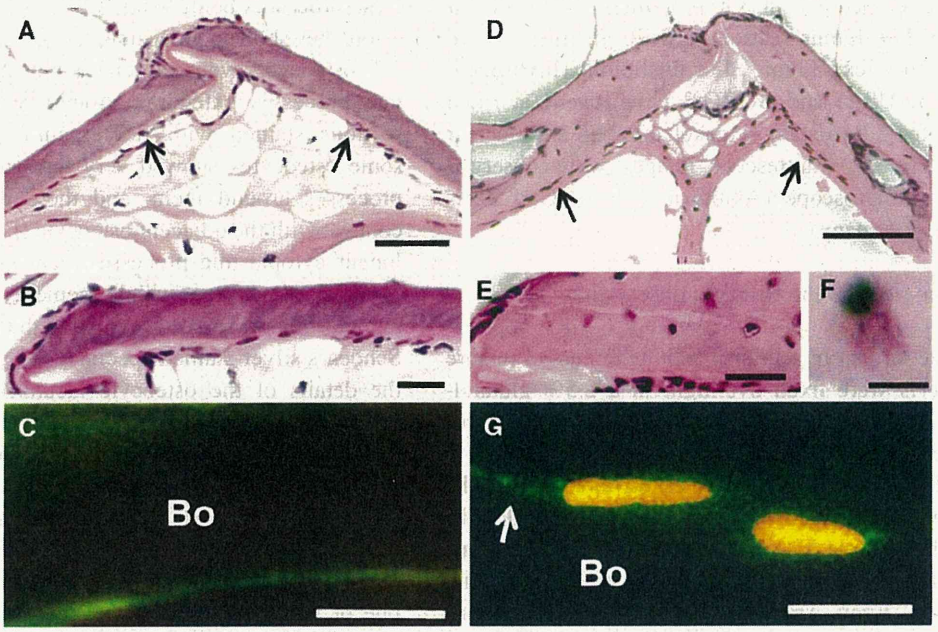

Fig. 1 Distribution of osteocytes and lacunocanalicular systems in medaka (**a–c**) and zebrafish (**d–g**). Low magnification of the centrum (vertebral body) in medaka (**a**) and zebrafish (**d**), and higher magnification pictures in medaka (**b**) and zebrafish (**e**, **f**). A thin layer of osteoblastic cells covered the surface of these bony elements (*arrows* in **a**, **d**). Note that no osteocytes are observed in medaka bone and osteocytes are observed in zebrafish bone. **a**, **b**, **d**, **e**, and **f** Schoen's silver staining. Scarcely stained osteocyte cell processes are observed in zebrafish bone (**d**, **e**), but cytoplasmic processes are rarely observed in some osteocytes (**f**). **c**, **g** Fluorescein-conjugated phalloidin-stained section. No osteocytes are seen in bone (*Bo*) of medaka in the section stained with fluorescein-conjugated phalloidin (**c**). Osteocytes observed in zebrafish show fine and short cytoplasmic processes around osteocytes, and a long cytoplasmic process (*white arrow*) is also observed in left osteocyte (**g**). *Orange* indicates the nuclei of osteocytes and *green* indicates the actin filaments stained with fluorescein-conjugated phalloidin in **g**. *Bars* 50 μm in **a** and **d**; 20 μm in **b** and **e**; 10 μm in **c**, **g**; 5 μm in **f**

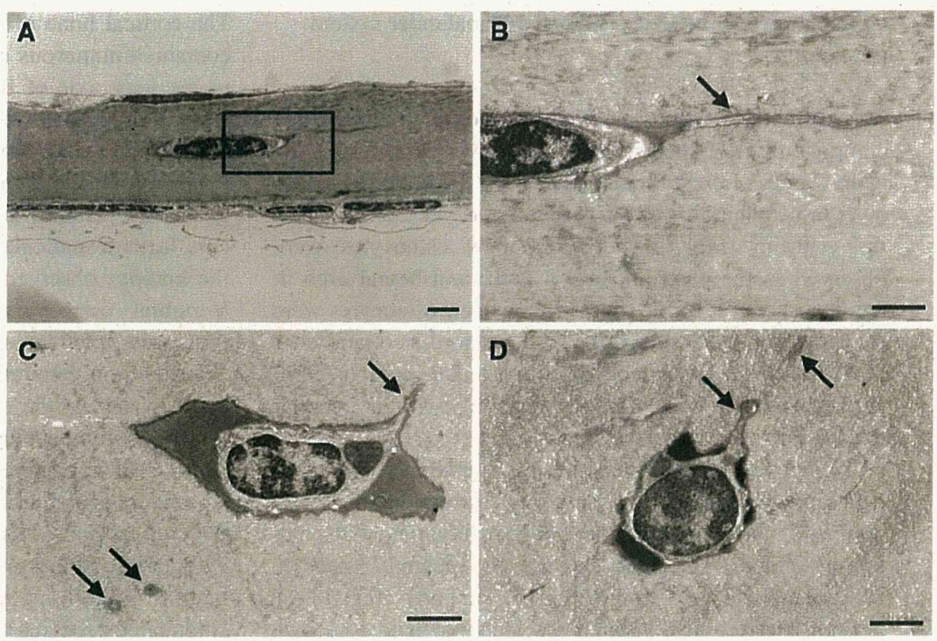

Fig. 2 Transmission electron micrographs of the centrum (vertebral body) in zebrafish. Low magnification of osteocytes and surrounding matrix (**a**). **b** Higher magnification of the rectangular region shown in **a**. Note that an osteocyte elongated a few cytoplasmic processes (*arrows*) into the surrounding matrix. Osteocytes extend a few cell processes into the matrix (*arrows* in **c**, **d**). The bone lacunae contain osteocytes and electron-dense substances showing different electron density (**c**, **d**). *Bars* 2 μm in **a**; 1 μm in **b** and **c**

shrunken osteocytes might be due to the fixation process. Taken together, the osteocyte lacunocanalicular system is more developed in *Xenopus laevis* than in the zebrafish.

Since *Xenopus laevis* is a water-living frog, we additionally investigated the distribution of osteocytes and the lacunocanalicular system in the cortical bones of the

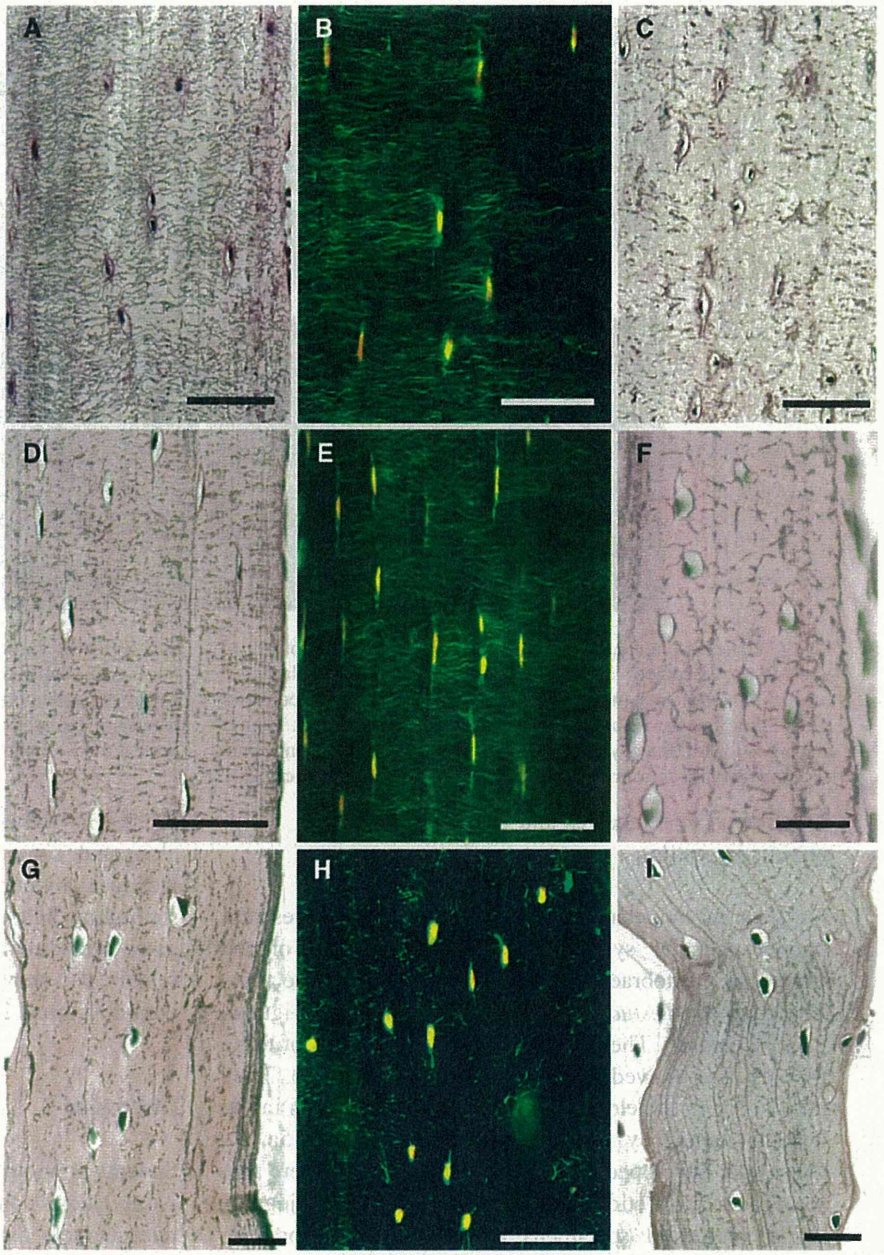

Fig. 3 Osteocyte lacunocanalicular system in mature *Xenopus laevis* (**a–c**). Cortical bone of femur in *Xenopus laevis* shows elongated osteocytes and a well-organized lacunocanalicular system in the sections stained with Schoen's silver staining (**a**) and fluorescein-conjugated phalloidin staining (**b**). Well-developed osteocyte lacunocanalicular system is seen in vertebrae of mature *Xenopus laevis* in the section stained by Schoen's silver method (**c**). Osteocyte lacunocanalicular systems in *Rana nigromaculata* (**d–f**). Sections from femurs of *Rana nigromaculata* stained with Schoen's silver method (**d**) and fluorescein-conjugated phalloidin (**e**). **f** Vertebral section of *Rana nigromaculata* stained by Schoen's silver method. Osteocyte lacunocanalicular system in *Cynops pyrrhogaster* (**g–i**). **g**, **h** Sections from femurs stained by Schoen's silver method and fluorescein-conjugated phalloidin, respectively. **i** Vertebral section stained by Schoen's silver method. *Bars* 20 μm in **f**, **g** and **i**; 50 μm in **a–e**; 100 μm in **h**

femur of mature *Rana nigromaculata*, which lives in water and on land. We found that these cortical bones also exhibited numerous elongated osteocytes aligned parallel to the long axis of the femur (Fig. 3d). The osteocyte lacunocanalicular system in this frog was perpendicular to the long axis of the femur (Fig. 3d). These findings were also confirmed by fluorescein-conjugated phalloidin staining (Fig. 3e). The vertebral osteocytes of *Rana nigromaculata* showed extension of many cytoplasmic processes into the surrounding bone matrix (Fig. 3f). To compare this distribution of osteocytes and lacunocanalicular systems with those in other amphibians, we examined the cortical bone of the femurs of *Cynops pyrrhogaster* (Japanese fire-bellied newt). Osteocytes in the femurs had numerous cytoplasmic processes extending into the bone matrix by Schoen's silver staining method (Fig. 3g), but they showed no peculiar direction as observed in cortical bones of frogs (Fig. 3a, d). Fluorescein-conjugated phalloidin-stained specimens revealed a similar distribution pattern of the osteocyte lacunocanalicular system in the femur (Fig. 3h). Osteocytes in vertebrae also showed a well-developed osteocyte lacunocanalicular system in the sections stained by Schoen's silver method (Fig. 3i).

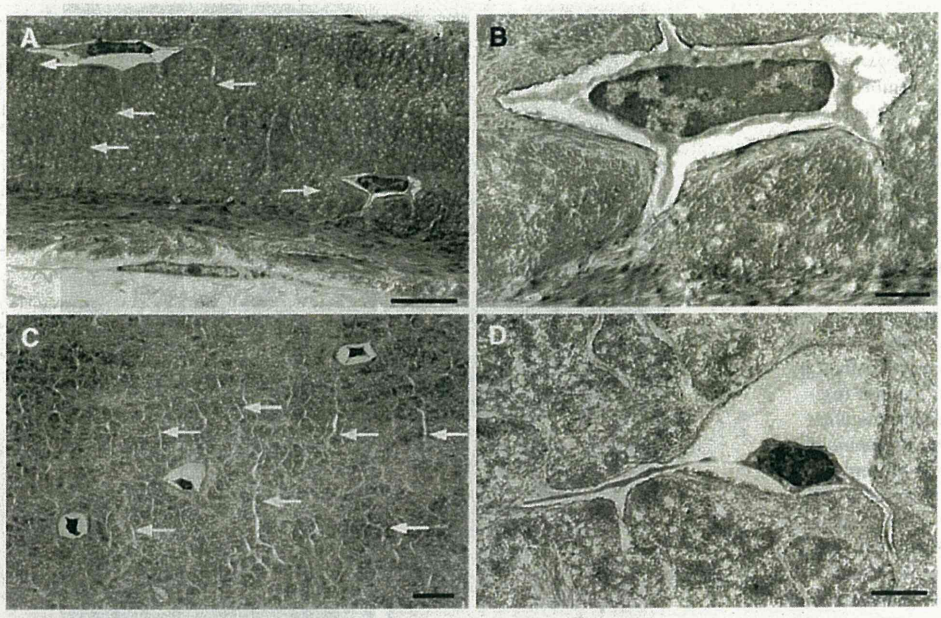

Fig. 4 Transmission electron micrographs of cortical bone of *Xenopus laevis*. Osteocytes and surrounding matrix at outer layer of cortical bone of femur (**a**, **b**). Note that an osteocyte elongated many cytoplasmic processes (*arrows*) into the surrounding matrix. Higher magnification of osteocyte shows well-developed cytoplasmic processes extending into bone matrix (**b**). Some osteocytes located at mid-region of cortical bones shows scanty cytoplasm and extended thick cytoplasmic processes into the bone matrix (*arrows* in **c**). The osteocyte lacuna containing shrunken osteocytes (**d**). This osteocyte extends cytoplasmic processes into the surrounding bone matrix (**d**). *Bars* 5 μm in **a** and **c**; 1 μm in **b**; 2 μm in **d**

Distribution of osteocytes and lacunocanalicular systems in reptiles

We then investigated the distribution of osteocytes and lacunocanalicular systems in the cortical bone of the femurs and vertebrae of two species of reptiles, the four-toed tortoise (*Testudo horsfieldii*) and the green iguana (*Iguana iguana*). The cortical bones of the femurs of these animals also showed numerous osteocytes (Fig. 5). They exhibited well-developed lacunocanalicular systems in the sections stained by Schoen's silver method (Fig. 5a, d). These well-developed lacunocanalicular systems were also observed in the section stained with fluorescein-conjugated phalloidin-stained specimens (Fig. 5b, e). Vertebrae in these animals also showed well-developed osteocyte lacunocanalicular systems (Fig. 5c, f). The sections stained by Schoen's silver method in these animals often showed osteocyte lacunae without any cell (empty lacunae) (Fig. 5c, d, f). These findings are due to artifacts during staining, because frozen sections used for fluorescein-conjugated phalloidin staining showed a few empty lacunae (Fig. 5b, e).

Distribution of osteocytes and lacunocanalicular systems in mammals

Finally, we investigated the distribution of osteocytes and lacunocanalicular systems in mammals. As shown in Fig. 6a, b, the cortical bone of the mouse had numerous elongated osteocytes associated with a well-developed lacunocanalicular system; this was seen in both sections stained by Schoen's silver method and fluorescein-conjugated phalloidin. Human cortical bones obtained from the femurs also showed numerous elongated osteocytes with a well-developed lacunocanalicular system (Fig. 6c).

Discussion

Several previous studies demonstrated that bone tissue in basal teleosts contains osteocytes, whereas that in advanced teleosts lacks osteocytes [11–13, 23]. In the present study, we confirmed these findings in the zebrafish (basal teleost) and medaka (advanced teleost). Previous morphological studies on osteocytes in basal teleosts, however, provide little information about the osteocyte lacunocanalicular system. To investigate the details of the osteocyte lacunocanalicular system in the zebrafish, we used Schoen's silver staining [22], actin filament staining with fluorescein-conjugated phalloidin, and transmission electron microscopy. In the bones of zebrafish, we could not find a well-developed osteocyte lacunocanalicular system as observed in amphibians, reptiles and mammals by Schoen's silver staining method, while fluorescein-conjugated phalloidin staining revealed that zebrafish osteocytes contained fine cytoplasmic processes, which seemed to

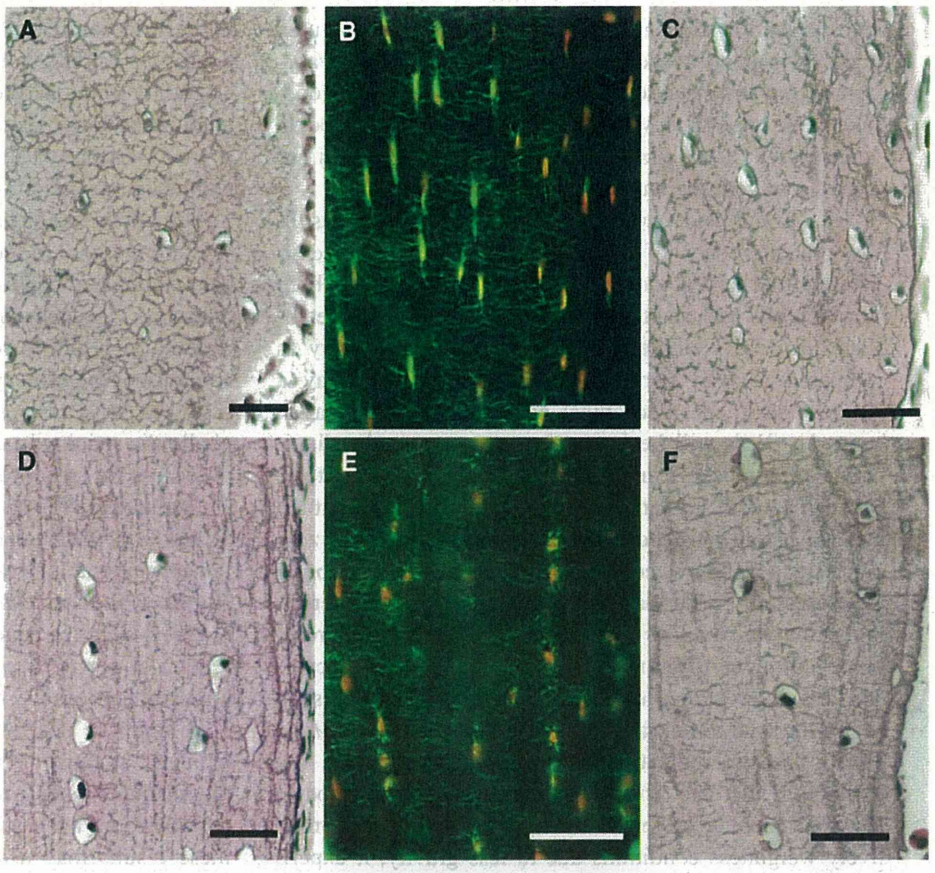

Fig. 5 Distribution of osteocytes and the lacunocanalicular system in the cortical bones of the femurs (**a**, **b**, **d**, **e**) and vertebrae (**c**, **f**) in four-toed tortoise (*Testudo horsfieldii*) (**a**–**c**) and green iguana (*Iguana iguana*) (**d**–**f**). Sections in **a**, **c**, **d**, and **f** were stained by Schoen's silver method, and those in **b** and **e** were stained with fluorescein-conjugated phalloidin. *Bars* 20 μm in **a**, **c**, **d** and **e**; 50 μm in **b** and **e**

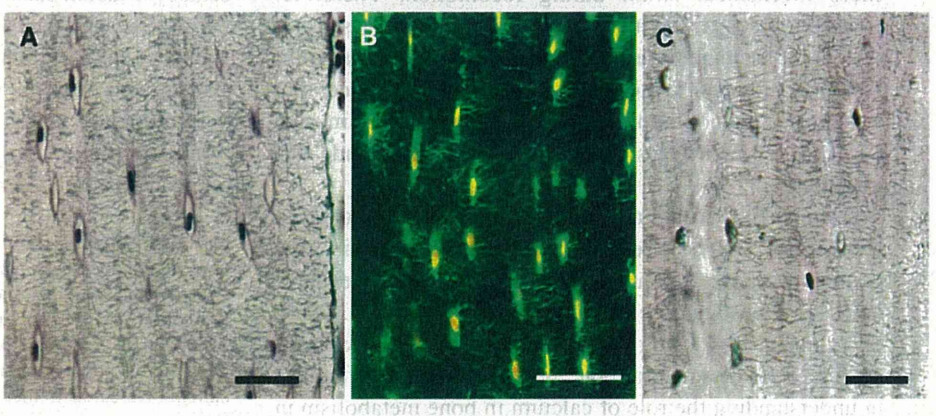

Fig. 6 Distribution of osteocytes and the lacunocanalicular system in cortical bone of the femur in mouse (**a**, **b**), and human (**c**). Sections in **a** and **c** were stained by Schoen's silver method, and that in **b** was stained with fluorescein-conjugated phalloidin. *Bars* 20 μm in **a** and **c**; 50 μm in **b**

connect with the adjacent osteocytes. On the other hand, thick and long cytoplasmic processes that were observed in the osteocyte lacunocanalicular system of other animals were rarely observed in zebrafish osteocytes by Schoen's silver staining, fluorescein-conjugated phalloidin staining, or electron microscopy (Figs. 1f, g, 2). The number of these cytoplasmic processes in zebrafish is limited to one or two in each osteocyte, while osteocytes in other animals exhibited numerous such structures. These results suggest that zebrafish bones have a poorly developed osteocyte lacunocanalicular system, compared to that in amphibians, reptiles, and mammals. Since zebrafish possess only the vertebral bone, we also compared the osteocyte lacunocanalicular system between vertebral bones and femurs in other animals. The vertebrae in these animals also retained well-developed osteocyte lacunocanalicular systems as well as femurs. These results indicate that a poorly developed osteocyte lacunocanalicular system in the zebrafish is not due to the difference between vertebral bone and long bone.

We showed the accumulation of an eosinophilic substance around some osteocytes in the sections of zebrafish

bones stained by Schoen's silver method. These structures might correspond to the amorphous substances with varying electron densities seen under the electron microscope. Since these structures were never observed in the osteocyte lacunae of *Xenopus laevis* and mouse, further studies are needed to reveal the nature of these substances.

Aquatic and land vertebrates live in different habitats. In this context, bones of these vertebrates are exposed to different mechanical strains and mineral acquisitions, both of which are important factors in regulating bone metabolism. Aquatic vertebrates are less affected by gravity as compared to land vertebrates. Since osteocytes play a central role in the mechanical adaptation of mammalian bones [1, 3], it will be interesting to compare the distribution of osteocytes and their lacunocanalicular systems between aquatic and land vertebrates. We revealed that the medaka has few osteocytes (acellular bone) and the zebrafish has apparent osteocytes (cellular bone) with a poorly developed osteocyte lacunocanalicular system. Interestingly, mature *Xenopus laevis*, which lives only in freshwater during its lifetime, exhibited numerous osteocytes and a well-developed osteocyte lacunocanalicular system as did the land vertebrates including *Rana nigromaculata*. These findings indicate that an aquatic habitat is not directly related to the development of an osteocyte lacunocanalicular system. Although the fish lives in relatively weightless conditions due to less gravity, it experiences mechanical strain during locomotion. Therefore, bones in teleost fishes may possess a mechanical sensing system other than osteocytes and the lacunocanalicular system. Although Witten and Huysseune suggested that osteoblasts and bone-lining cells might be involved in such a system [13], further studies are needed to conclude this hypothesis.

Bone plays vital roles in calcium and phosphate metabolism and is a reservoir of these minerals in land vertebrates; however, such functions in teleost bones have not been investigated extensively. In this context, Moss's experiments [24] using a fracture model of teleosts with cellular bone or acellular bone provide interesting findings in understanding the role of calcium in bone metabolism in teleost fishes. When goldfish (*Carassius auratus*), which has a cellular bone, and tilapia (*Tilapia macrocephala*), which has an acellular bone, were kept in calcium-depleted water, the goldfish formed a fracture callus composed of calcified cartilage and bone, but the tilapia formed uncalcified cartilage callus during fracture repair. These results suggest that calcium mobilization from bone is limited in teleost fishes with acellular bones and supports the idea that osteocytes play some role in calcium mobilization.

We conducted a comparative study on the morphology of the osteocyte lacunocanalicular system in the bones of various vertebrates by using Schoen's silver staining and fluorescein-conjugated phalloidin methods. In zebrafish bones, we observed fine and short cytoplasmic processes extending from the osteocytes in the fluorescein-conjugated phalloidin stained specimens, but not in the Schoen's silver-stained sections. These results suggest that fluorescein-conjugated phalloidin staining is more sensitive in detecting fine osteocyte cytoplasmic processes than Schoen's silver staining method. In the bones of other vertebrates, fluorescein-conjugated phalloidin staining clearly demonstrated an osteocyte lacunocanalicular system. Furthermore, this staining also allows observation of the three-dimensional structure of the osteocyte lacunocanalicular system under a confocal laser microscope. Thus, fluorescein-conjugated phalloidin staining is a useful technique to observe details of the osteocyte lacunocanalicular system.

Our study revealed that amphibians and land vertebrates possess a well-developed osteocyte lacunocanalicular system. Among amphibians, femurs of frogs (*Xenopus laevis* and *Rana nigromaculata*) exhibited osteocyte lacunocanalicular systems arranged perpendicular to the long axis, but femurs of newts (*Cynops pyrrhogaster*) showed a random arrangement of the osteocyte lacunocanalicular system. This might be due to the different maturation stage of the animals, because Hirose et al. [22] reported that the alignment of osteocyte lacunocanalicular systems changed depending on the maturation stages of mice. Alternatively, these results may also suggest that the alignment of the osteocyte lacunocanalicular systems may differ among the various species of vertebrates. In this context, further studies on the structure of osteocyte lacunocanalicular systems of various vertebrates, including the different developmental stages of each species, will provide more information and help to understand the phylogenic development and function of osteocytes.

Acknowledgments We thank Dr. Shizuko Ichinose and Dr. Akiko Himeno for their technical assistance. This work was supported by Grant-in-Aid for Scientific Research from the Japan Society for the Promotion of Science (14104015 and 22249061 to A.Y. and 21659426 to T.I.) and by a grant from the Japanese Ministry of Education, Global Center of Excellence (GCOE) Program, "International Research Center for Molecular Science in Tooth and Bone Diseases".

References

1. Bonewald LF (2006) Mechanosensation and transduction in osteocytes. Bonekey Osteovision 3:7–15
2. Tatsumi S, Ishii K, Amizuka N, Li M, Kobayashi T, Kohno K, Ito M, Takeshita S, Ikeda K (2007) Targeted ablation of osteocytes induces osteoporosis with defective mechanotransduction. Cell Metab 5:464–475
3. Henriksen K, Neutzsky-Wulff AV, Bonewald LF, Karsdal MA (2009) Local communication on and within bone controls bone remodeling. Bone 44:1026–1033